

**THE UNIVERSITY OF TURKISH AERONAUTICAL ASSOCIATION  
INSTITUTE OF SCIENCE AND TECHNOLOGY**



**ESTIMATION OF EDDY CURRENT LOSSES IN METALLIC  
TRANSMISSION TOWERS**

**Master Thesis**

**Huda Mohammed**

**Electrical and Electronics Engineering Department**

**Master Thesis Program**

**January, 2017**

**THE UNIVERSITY OF TURKISH AERONAUTICAL ASSOCIATION  
INSTITUTE OF SCIENCE AND TECHNOLOGY**



**ESTIMATION OF EDDY CURRENT LOSSES IN METALLIC  
TRANSMISSION TOWERS**

**MASTER THESIS**

**Huda Mohammed**

**1403630008**

**Electrical and Electronics Department**

**Master Thesis Program**

**Supervisor: Assist. Prof. Dr. Ibrahim Mahariq**

Huda MOHAMMED, having student number 1403630008 and enrolled in the Master Program at the Institute of Science and Technology at the University of Turkish Aeronautical Association, after meeting all of the required conditions contained in the related regulations, has successfully accomplished, in front of the jury, the presentation of the thesis prepared with the title of: Estimation of Eddy Current Losses in Metallic Transmission Towers.

**Supervisor:**

  
Assist. Prof. Dr. Ibrahim MAHARIQ

The University of Turkish Aeronautical Association

**Jury Members:**

Prof. Dr. Mehmet AYDEMIR



Gazi University

  
Assist. Prof. Dr. Hassan SHARABATY

The University of Turkish Aeronautical Association

**Thesis Defense Date:** 26.01.2017

**THE UNIVERSITY OF TURKISH AERONAUTICAL ASSOCIATION  
INSTITUTE OF SCIENCE AND TECHNOLOGY**

**I hereby declare that all the information in this study I presented as my Master's Thesis, called "Estimation of Eddy Current Losses in Metallic Transmission Towers" has been presented in accordance with the academic rules and ethical conduct. I also declare and certify on my honor that I have fully cited and referenced all the sources I made use of in this present study.**

**Date 11/01/2017**

**Huda Mohammed**



## **ACKNOWLEDGEMENTS**

First of all I am grateful to The Almighty Allah for helping me to complete this thesis.

I would like to express gratitude to my supervisor, Assist. Prof. Dr. Ibrahim Mahariq, for his patience, encouragement, useful advice, discussion, comments and understanding my situation. He gave me opportunities to present my work in front of experts in the field.

I would like also to express my special thanks to Mrs. Hadeel for her useful advices and notes.

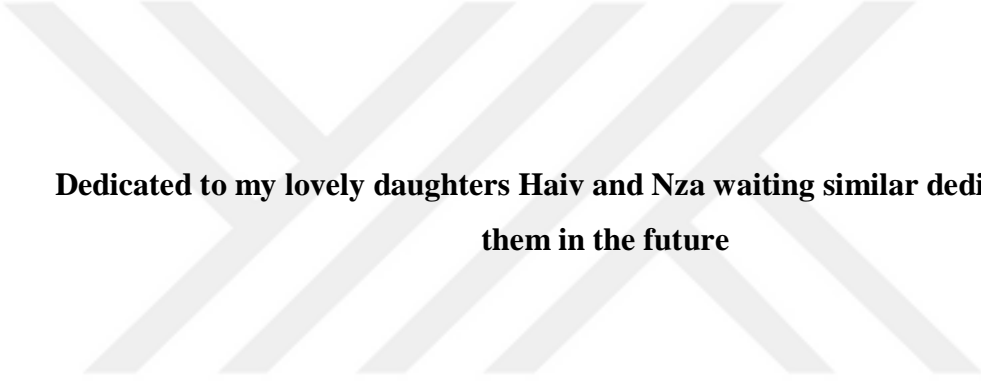
I am forever profoundly indebted to my parents, for their supports, without their prayers the completion of this thesis would not have been possible.

Thanks to my sister, brothers, family and friends.

I would like to express my profound gratitude to my daughters Haiv and Nza, to whom this work is dedicated, for every time they needed me but I wasn't there. For missing me throughout my study.

The most of all my sincere love and infinite appreciation goes to my husband, Rahell MR., for being everything in my life, for his patience, supporting, invaluable assistance, for every time he listened to me when reviewing the thesis.

**Huda Mohammed**



**Dedicated to my lovely daughters Haiv and Nza waiting similar dedications from  
them in the future**

## Table of Contents

<b>TABLE OF FIGURS .....</b>	<b>VI</b>
<b>List of characters.....</b>	<b>X</b>
<b>ABSTRACT.....</b>	<b>XI</b>
<b>ÖZET .....</b>	<b>XIII</b>
<b>CHAPTER ONE .....</b>	<b>1</b>
<b>INTRODUCTION .....</b>	<b>1</b>
<b>1.1 General overview .....</b>	<b>1</b>
<b>1.2 Literature overview .....</b>	<b>3</b>
<b>1.2.1 Technical and non-technical losses.....</b>	<b>3</b>
<b>1.2.2 Transmission lines magnetic field.....</b>	<b>4</b>
<b>1.2.3 Numerical methods and boundary conditions .....</b>	<b>7</b>
<b>1.3 Thesis objectives .....</b>	<b>8</b>
<b>1.4 Significance of this thesis .....</b>	<b>8</b>
<b>1.5 Arrangement of this thesis.....</b>	<b>9</b>
<b>CHAPTER TWO .....</b>	<b>10</b>
<b>CHALLENGES ASSOCIATED WITH POWER TRANSMISSION .....</b>	<b>10</b>
<b>2.1 Modeling of Transmission lines .....</b>	<b>10</b>
<b>2.1.1 Short transmission lines. ....</b>	<b>10</b>
<b>2.1.2 Medium transmission lines.....</b>	<b>11</b>
<b>2.1.3 Long transmission lines .....</b>	<b>12</b>
<b>2.2 Transmission towers .....</b>	<b>13</b>
<b>2.2.1 AC transmission towers.....</b>	<b>13</b>
<b>2.2.2 DC transmission towers.....</b>	<b>14</b>

2.2.3	Towers of AC railway traction line .....	15
2.2.4	Design of towers (transmission and distribution) .....	15
2.2.5	Materials of transmission towers.....	17
2.3	Losses in transmission line .....	19
2.3.1	Technical losses .....	20
2.3.2	Non-technical losses .....	21
2.4	Transmission efficiency.....	22
<b>CHAPTER THREE .....</b>		<b>23</b>
<b>MAGNETIC FIELD AND PROBLEM DEFINITION.....</b>		<b>23</b>
3.1	Magnetic field around transmission lines .....	23
3.1.1	Biot-savart law .....	24
3.1.2	Ampere's Circuital Law .....	25
3.2	Eddy current formulation .....	26
3.2.1	Faraday's Law.....	27
3.2.2	Lenz's Law.....	27
3.3	Maxwell's equation .....	28
3.3.1	Gauss's law for electricity .....	28
3.3.2	Gauss's law for magnetism .....	29
3.3.3	Faraday's law of induction.....	29
3.3.4	Maxwell's form of Ampere's circuital law .....	30
3.4	Numerical methods .....	31
3.4.1	Finite difference method FDM.....	31
3.4.2	Finite element method FEM.....	32
3.4.3	Charge simulation method .....	33
3.4.4	Boundary element method .....	33



3.5	Boundary and interface conditions.....	34
3.6	Problem formulation.....	35
3.6.1	Differential equation derivation .....	36
3.7	Problem formulation by FDM .....	41
<b>CHAPTER FOUR.....</b>		<b>43</b>
<b>RESULTS AND DISCUSSION.....</b>		<b>43</b>
4.1	Computational domain and boundary conditions.....	43
4.2	Magnetic vector potential .....	45
4.3	Eddy current and eddy current losses.....	47
4.3.1	Permeability of the transmission tower .....	48
4.3.2	The distance to the source current .....	49
4.3.3	Conductivity of the transmission tower .....	52
4.3.4	Dimensions of the computed area.....	53
4.3.5	Excitation current .....	55
4.3.6	Maximum current.....	60
4.3.7	Frequency of the excitation current .....	62
<b>CHAPTER FIVE .....</b>		<b>63</b>
<b>CONCLUSIONS AND FUTURE WORK.....</b>		<b>63</b>
5.1	Conclusion.....	63
	Future Work .....	64
<b>References.....</b>		<b>65</b>

## TABLE OF FIGURS

Figure 1.1: A typical power system representation.....	2
Figure 1.2: magnetic flux density under 500Kv [33].....	5
Figure 1.3: Distribution of magnetic field lines around 400 kV line [36] .....	6
Figure 2.1: Equivalent circuit of short transmission line [12]. .....	11
Figure 2.2: Equivalent circuit of medium-length line T-circuit [12] .....	12
Figure 2.3: Equivalent circuit of medium-length line $\pi$ -circuit [12]. .....	12
Figure 2.4: Equivalent circuit of long-length line [12]. .....	13
Figure 2.5: A typical high voltage AC transmission tower .....	14
Figure 2.6: DC transmission tower. ....	15
Figure 2.7: Wooden pole of A and H-type.....	17
Figure 2.8: RCC towers .....	18
Figure 2.9: A steel lattice tower.....	19
Figure 3.1: Magnetic field lines around a current carrying conductor [22] .....	24
Figure 3.2: Biot-savart law .....	25
Figure 3.3: Ampere circuital law .....	26
Figure 3.4: The induction of eddy currents.....	27
Figure 3.5: Gauss's law for electricity .....	28
Figure 3.6: Gauss's law for magnetism .....	29
Figure 3.7: Faraday's law of induction.....	30
Figure 3.8: Ampere's circuital law .....	30
Figure 3.9: Discritazation of the computational domain by FDM grid .....	31
Figure 3.10: Finite element method .....	33
Figure 3.11: CSM using ring charges .....	33

Figure 3.12: CSM using point charges .....	33
Figure 3.13: Discretization of the boundary for BEM [47] .....	34
Figure 3.14: The geometry of the problem .....	38
Figure 3.15: Interface condition.....	40
Figure 3.16: Reduced computational domain .....	41
Figure 3.17: Problem formulation by FDM .....	41
Figure 3.18: Five stencil FDM cell .....	42
Figure 3.19: Interface boundary node .....	42
Figure 4.1: Eddy current .....	44
Figure 4.2: the impact of d on the calculation of the eddy current .....	44
Figure 4.3: The influence of d on the eddy currents in the upper side nodes of the metallic square .....	45
Figure 4.4: Magnetic vector potential at $I=500A$ , $\mu = 200\mu_0$ , $\sigma = 200S/m$ for maximum current through the middle phase.....	46
Figure 4.5 Magnetic vector potential at $I=500A$ , $\mu = 200\mu_0$ , $\sigma = 200S/m$ when maximum current passes through the left phase.....	46
Figure 4.6 Magnetic vector potential at $I=500A$ , $\mu = 200\mu_0$ , $\sigma = 200S/m$ when maximum current passes through the right phase.....	47
Figure 4.7 Eddy current at $I=500A$ , $\mu = 200\mu_0$ , $\sigma = 200S/m$ .....	47
Figure 4.8 the influence of metals permeability on the induced eddy current. a) The eddy current for metal with property of ( $\mu = 30\mu_0$ ). b) The eddy current for metal with property of ( $\mu = 20\mu_0$ ). c) The eddy current for metal with property of ( $\mu = 15\mu_0$ ), d) The eddy current for metal with property of ( $\mu = 5\mu_0$ ).....	48
Figure 4.9: The relationship between the permeability and the induced eddy current ....	49
Figure 4.10 Eddy currents at different distances from the source for with ( $\mu = 5\mu_0$ , $\sigma = 10000S/m$ , $I = 500A$ ): a) 0.5m. b) 0.8m c) 1m. d) 1.5m. ....	50

Figure 4.11: The relationship between the eddy current and the distance from the source .....	51
Figure 4.12: Eddy current at different distance from the source for with ( $\mu = 5\mu_0, \sigma = 10000\text{S/m}, I = 500\text{A}$ ): a) 0.5m. b) 0.8m c) 1m. d) 1.5m. ....	51
Figure 4.13: The influence of metals conductivity on the induced eddy current. a) The eddy current for metal with property of ( $\sigma = 100\text{S/m}$ ). b) The eddy current for metal with property of ( $\sigma = 500\text{S/m}$ ). c) The eddy current for metal with property of ( $\sigma = 1000\text{S/m}$ , d) The eddy current for metal with property of ( $\sigma = 10000\text{S/m}$ .....	52
Figure 4.14: The relationship between the eddy current and metal conductivity. ....	53
Figure 4.15: Eddy current for $2\text{cm} \times 2\text{cm}$ with ( $\mu = 5\mu_0, \sigma = 10000\text{S/m}, I = 500\text{A}$ )	54
Figure 4.16: Eddy current for $3\text{cm} \times 3\text{cm}$ with ( $\mu = 5\mu_0, \sigma = 10000\text{S/m}, I = 500\text{A}$ )	54
Figure 4.17: Eddy current for $4\text{cm} \times 4\text{cm}$ with ( $\mu = 5\mu_0, \sigma = 10000\text{S/m}, I = 500\text{A}$ )	55
Figure 4.18: Eddy current for $4\text{cm} \times 4\text{cm}$ with ( $\mu = 5\mu_0, \sigma = 10000\text{S/m}, I = 10000\text{A}$ ) when the distance between phases is 1m. ....	56
Figure 4.19: Eddy current for $4\text{cm} \times 4\text{cm}$ with ( $\mu = 5\mu_0, \sigma = 10000\text{S/m}, I = 10000\text{A}$ ) when the distance between phases is 0.5m. ....	56
Figure 4.20: Eddy current for $4\text{cm} \times 4\text{cm}$ with ( $\mu = 5\mu_0, \sigma = 10000\text{S/m}, I = 1000\text{A}$ ) when the distance between phases is 1m. ....	57
Figure 4.21: Eddy current for $4\text{cm} \times 4\text{cm}$ with ( $\mu = 5\mu_0, \sigma = 10000\text{S/m}, I = 1000\text{A}$ ) when the distance between phases is 0.5m. ....	57
Figure 4.22: Eddy current for $4\text{cm} \times 4\text{cm}$ with ( $\mu = 5\mu_0, \sigma = 10000\text{S/m}, I = 500\text{A}$ ) when the distance between phases is 0.5m. ....	58
Figure 4.23: Eddy current with ( $\mu = 5\mu_0, \sigma = 10000\text{S/m}, I = 500\text{A}$ ) when the distance between phases is 1m.....	59
Figure 4.24: The relationship between the eddy current and the excitation current.....	59
Figure 4.25: Eddy current in the metal with ( $\mu = 5\mu_0, \sigma = 10000\text{S/m}$ ) considering the instant that a maximum current of 500A passes through the middle phase. ....	60

Figure 4.26: Eddy current in the metal with ( $\mu = 5\mu_0, \sigma = 10000\text{S/m}$ ) considering the instant that a maximum current of 500A passes through the left phase. ....61

Figure 4.27: Eddy current in the metal with ( $\mu = 5\mu_0, \sigma = 10000\text{S/m}$ ) considering the instant that a maximum current of 500A passes through the right phase. ....61



## List of characters

FDM	Finite difference method
FEM	Finite element method
CSM	Charge simulation method
BEM	Boundary element method
PDE	Partial differential equation
$P_e$	Eddy current losses
$\sigma$	Electrical conductivity
$J$	Current density
$B$	Magnetic flux density
$H$	Magnetic field intensity
$\omega$	Angular frequency
$\mu$	permeability
$\mu_0$	Permeability of the free space
$A$	Magnetic vector potential
$D$	Electric displacement field/ electrical flux density
$E$	Electric field
RCC	Reinforced concrete poles
EMDEX II	Electric and magnetic field digital exposure
$I$	Electrical current
$\rho$	Electrical charge density
$q$	Electric charge
$V$	Electric potential voltage
$\eta$	Efficiency
$\epsilon_0$	Permittivity of the free space
PSO	Particle Swarm Optimization technique

## **ABSTRACT**

### **ESTIMATION OF EDDY CURRENT LOSSES IN METALLIC TRANSMISSION TOWERS**

MOHAMMED, Huda

Mater, Department of Electric and Electronic

Thesis supervisor: Assist. Prof. Dr. Ibrahim, MAMHARIQ

January–2017, 71 page

The existence of magnetic field around the high-voltage overhead transmission lines or the low-voltage distribution lines is a known fact and well-studied in the literature. Taking into consideration that many countries use metallic towers due to its advantage over other materials. However, the interaction of the magnetic field either with transmission or distribution towers has not been investigated. Noteworthy it is to remember that this field is time-varying low-frequency of 50Hz or 60Hz depending on the country. In this study, we report for the first time the existence of eddy currents in towers which are made of metals. As the geometrical structure of towers are extremely complex to model, we provide a simple model based on electromagnetism in order to verify the existence of power loss in the form of eddy currents. The frequency-domain finite difference method is adapted in the current study for the estimation of magnetic vector potential and hence eddy current losses in the tower. Our approach connects the magnetic calculation and the electric calculation by the introduction of Faraday's law in the electric field calculation. The equation of the magnetic field is determined and solved by the aid of finite difference method. The importance of such a study is the addition of a new type of power loss to the power network due to the fact that some towers are made of relatively conductive materials. Calculations made at different material properties hence

in addition to its mathematical modelling and importance to researchers interested in the field, this study provides important keys to towers manufacturers in selecting the proper materials so that the eddy current losses are minimum.

**Keywords:** Eddy current, finite difference method, metallic towers, power systems.





## ÖZET

### METAL İLETİM KULELERİNDE EDDY AKIMI YİTİMİ TAHMİNİ

Huda MUHAMMED

Elektrik ve Elektronik Bölümü

Tez Danışmanı: Yardımcı Doç. Dr. İbrahim MAHARİQ

Ocak-2017, 71 Sayfa

Yüksek voltajlı havai iletim hatları veya düşük voltajlı dağıtım hatları çevresinde manyetik alanın varlığı bilinen bir gerçektir ve literatürde oldukça çalışılmıştır. Pek çok ülkenin diğer materyallere göre avantajlı olması nedeniyle metal kuleler kullandığı göz önünde bulundurulmaktadır. Ancak manyetik alanın diğer iletim veya dağıtım kuleleriyle etkileşimi incelenmemiştir. Bu alanın, ülkeye bağlı olarak, zaman değişmeli alçak frekansının 50Hz veya 60Hz olduğunu hatırlamak önemlidir. Bu çalışmada ilk kez, metallerden yapılmış kulelerde eddy akımlarının varlığını anlatıyoruz. Kulelerin geometrik yapısı bir modelini yapmak için hayli karmaşık olduğundan, eddy akımlarında güç yitiminin varlığını doğrulamak amacıyla elektromanyetizmaya dayalı basit bir model sunuyoruz. Çalışmada, manyetik vektör potansiyelinin ve nihayetinde kuledeki eddy akımı yitiminin tahmin edilmesi için frekans dümeninde sonlu farklar yöntemi uyarlanmıştır. Yaklaşımımız, elektrik alanı hesaplamasında Faraday kanununu kullanarak manyetik hesaplama ile elektrik hesaplanmasını birleştirmektedir. Manyetik alan denklemi kurulup sonlu farklar yöntemi yardımıyla çözülmüştür. Böyle bir çalışmanın önemi, bazı kulelerin görece iletken materyallerden yapılması nedeniyle elektrik şebekesine yeni bir tür güç kaybı eklemesidir. Farklı materyal özelliklerinin hesaplanmasının yanı sıra matematiksel modellemesi ve bu alanla ilgilenen araştırmacılar için önemiyle birlikte bu çalışma, eddy akımı yitiminin minimuma indirilmesi için uygun materyaller seçme konusunda kule üreticilerine önemli noktalar sunmaktadır.

**Anahtar Kelimeler:** Eddy akımı, sonlu farklar yöntemi, metal kuleler, elektrik şebekeleri.

# CHAPTER ONE

## INTRODUCTION

### 1.1 General overview

The overhead transmission system is the biggest system in the world. Its function is to transport electric power from the supplier to the consumer. In a power system, there are several factors for energy losses. Some of energy generated and supplied to the distribution utility does not reach the end consumer. The generated power passes through different components with different materials and properties like transformers, cables and other equipment. This complex system causes energy losses in the power system. Regardless of how the power system is modeled and designed, losses exist. Initially the power losses in transmission and distribution are classified as technical and non-technical losses. Some of the energy is lost in the form of heat in the conductors, some are absorbed in insulating materials, and some of the energy is dissipated into a magnetic field [1].

As our concern here is the influence of magnetic field, the time varying electric current in transmission line conductor produces a concentric circles of magnetic field lines surrounding the conductor [2-5]. At any point around the transmission line the magnetic field intensity is described by a field vector which is perpendicular to the distance from the center of the line conductor. The generated magnetic field is a low frequency quasi-static field which the possibility of its influence on human and objects in the vicinity has been a serious concern recently. There are many researches on the environmental effect of the magnetic field and methods for minimizing the harmful magnetic field were developed because power transmission lines are mostly in the close vicinity of buildings [6, 7].

When talking about environment subjects that are effected by the magnetic field of transmission lines, it is worthy to shed light on the tower holding it too. Metallic towers

are largely used in power transmission and telecommunications applications. Most of electrical transmission towers in most of countries are made of steel due to its advantage over other materials as for its high mechanical strength withstanding bad climatic cases. In addition, steel needs less maintenance compared to other material types [8]. These towers are interacting with the magnetic field produced by the current carrying conductors of the three phase transmission line. The transmission tower has a complex design characterized in such a way that it meets the special needs from structural and electrical points of view. The design of the tower may change from one to another according to the company, the place of the tower and the load.

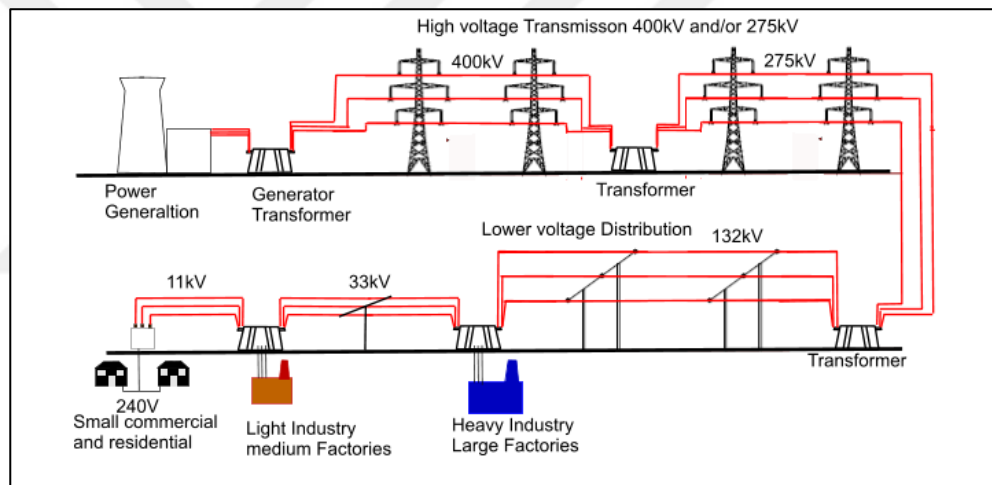


**Figure 1.1:** A typical power system representation

In this study we confirm on the existence of eddy-current losses in transmission towers under balanced condition. Although it is slight, especially at balanced conditions, eddy currents are calculated in the tower. By using the finite difference method for solving Maxwell's differential equations in low frequency domain, the resulting eddy-current losses in the tower at balanced condition are estimated at different material properties. Our approach connects the magnetic calculation and the electric calculation by the introduction of Faraday's law in the electric field calculation. Calculations start from Maxwell's equation describing the quasi-static magnetic field, the source current of the overhead lines, and approximate boundary conditions. The series equation of Maxwell's equations

are transformed by FDM's discretization to a system of linear algebraic equations from which the solution are calculated. The study provides a feasible mathematical modelling for calculating magnetic field and eddy current in addition to its importance to researchers interested in the field, this study provides important keys to towers manufacturers in selecting the proper materials so that minimum losses is occur due to eddy currents.

## **1.2 Literature overview**

Metallic towers are widely used in transmission and telecommunication systems. Steel towers are largely used in power transmission systems because of its high mechanical strength withstanding bad climatic cases [9]. In addition, steel needs less maintenance compared to other material types. The function of metallic towers is to support the power lines that has a complex design constructed in a way to meet the special needs from structural and electrical points of view [10] with the consideration of construction demand as they constitute about 28% to 42% of the cost of transmission line [11]. The design of the tower may change from one to other according to the company, the place of the tower and the load [12]. These metallic towers interacts with power lines magnetic field produced by the current flow of the three phase transmission line.

Transmission lines losses and information about methods and software used in previous researches for the calculation of magnetic field are presented in the previous and the following references to which the reader may refer for details. The transmission of electric power is associated with magnetic induction. Some of the magnetic field is dissipated in environment objects. The dissipated magnetic field is considered as one of the factors that causes energy losses in the power system.

### **1.2.1 Technical and non-technical losses**

As the power flows in the transmission and distribution network, a substantial amount of the generated energy is lost in the system. The power losses are classified as technical losses caused by internal factors [13] and non-technical losses caused by external factors [14]. The analysis of power system losses has been one of concerns because of its economic and environmental impacts. Many methods were presented in the literature for losses calculation [15] and other researches dedicated on methods to minimize the

wasteful energy as much as possible to improve the power system efficiency and hence saving the wasted cost due to energy losses [1, 16, 17]. The average transmission line losses can be expressed by [14]:

$$P_{losses} = P_{source} - P_{load} \quad 1.1$$

where  $P_{source}$  is the average power generated and supplied to the transmission system, and  $P_{load}$  is the average power delivered by transmission line and consumed at the load end.

### 1.2.2 Transmission lines magnetic field

Electromagnetic fields around overhead power lines are produced due to the current and voltage of transmission lines conductor [2, 5, 18, 19] this electromagnetic fields may effect humans and objects in the vicinity [20, 21]. To measure the produced magnetic field from overhead lines hence determining the phase current and line position, magnetoresistive sensors can be proposed in the ground level [22, 23]. Magnetic sensors can be also used to determine a magnetic field security zone to prevent interference with electric equipment in the vicinity of high voltage power lines [7] because the produced magnetic field around the conductors of transmission lines reduces as the distance from the tower increases [6]. So the influence of the magnetic field on human depends on humans position from the power line [24], that's why high voltage transmission towers should not be located near residential areas as much as possible. Although there are no concrete evidence that the emitted magnetic field is harmful however, researchers are concerned about it. Ref [25] discusses the biological effect of the magnetic field using EMDEX II for the measurement of the magnetic field for 132Kv overhead lines. The structural steel that always run parallel to the three phase line which is used to provide mechanical protection for the current lines is an example of the magnetic field influence which may produce eddy currents in the structural steel [26]. The effect of the magnetic field on the maintenance personnel and how different type of towers have different susceptibility to electromagnetic field is discussed in [4], where the author illustrates that the geometry of the one-circuit Y shaped tower is less favorable than the barrel two-circuit tower. Also, climbing routes which are used for maintenance purposes were analyzed and

the electric and magnetic fields are calculated. All the electric and magnetic field calculations can be used for any shape of electric structure. Ref. [27] Presents the interaction between the conductors of the transmission lines and the holding tower by studying the effect of the number of infinite line charges per conductor of the overhead lines. While the effect of the tower configurations along the insulator was investigated in [28].

The harmful magnetic field can be minimized according to the place of the conductor in space using phase split arrangements, active and passive shielding, passive circuits can be useful for the reduction of the harmful magnetic field for instance but not limited to. The PSO can be used to find the best arrangement of the phases that gives the minimum electromagnetic field [29-32].

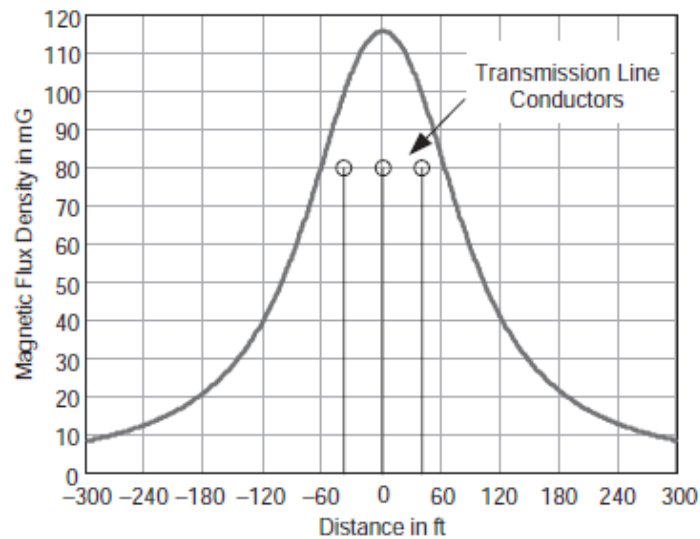


**Figure 1.2:** magnetic flux density under 500Kv [33]

The magnetic field of transmission line can be considered as quasi-static field because of the influence of low frequency. The calculation starts with the low frequency limit of Maxwell's equation [34]. Different numerical methods can be applied for the calculation of the magnetic field, one of the method used is finite difference method FDM by solving Maxwell's equation also the effect of supply frequency, resistivity, and bus height on the calculation can be considered [35], finite element method (FEM) is also a common method for magnetic field calculations [28, 36, 37]. While [4] uses boundary

element method BEM. Another method is charge simulation method CSM [38] in which the tower and the phase conductors are divided into short segments and solved as presented in [39]. Ref. [40] uses exact and approximate methods for analyzing the magnetic field around the overhead power lines, obtaining magnetic field in the free space from Biot-Savart law, the influence of earth current on the magnetic field above the surface of the earth can be neglected when compared with the currents flowing in the overhead conductors. The analytical formula of the magnetic field is presented by complex numbers as shown in [3].

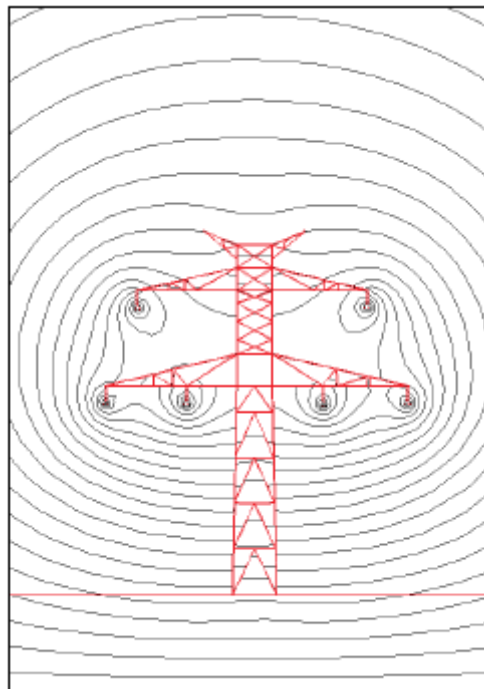


**Figure 1.3:** Distribution of magnetic field lines around 400 kV line [36]

The basic laws of eddy currents are Faraday's and Lenz's law [41]. The source current, frequency, the distance from the current source to the induced eddy current media and the geometry of the conducting sample where eddy currents are induced all of them are factors affecting eddy current. As it is not easy to use an analytical method for the eddy currents induced in conducting materials by time varying magnetic field, most of researches dealing with a current-carrying problems uses Poisson's equation for finding the magnetic vector potential with the well-defined source current density [34]. The same

thing is used in [42] for eddy current problems by determining the current density and obtaining the losses by evaluating it by the volume integral method. The formulation of eddy currents and interface boundary conditions are described briefly in [43, 44]. Starting with the derivation of Maxwell's equation for the quasi-static magnetic field, one can obtain the governing equation for eddy current calculations [43-45].

There are two ways for calculating eddy current losses first by evaluating the volume integral of the eddy current density [42]:

$$p_e = \int_v \frac{\vec{J}_e \cdot \vec{J}_e^*}{\sigma} \quad 1.2$$

where  $p_e$  is the eddy current losses,  $J_e$  is the eddy current density,  $J_e^*$  indicates the complex conjugate of the eddy current density.

The second method is to determine the source impedance evaluating the eddy current losses by:

$$p_e = I_{rms}^2 \cdot \text{real} \left[ \frac{-j\omega \vec{A}(0, h)}{I} \right] \quad 1.3$$

where  $I$  is the source current,  $A$  is the magnetic vector potential,  $\omega$  is the angular frequency,  $h$  is the distance between the source and the conducting material,

### 1.2.3 Numerical methods and boundary conditions

Most of partial differential equations of electromagnetic problems do not have analytical solutions so the approximate solution of the partial differential equation is found by numerical methods [46]. FDM is a common method used in linear problems of time dependence with regular geometry. FEM is used in linear and nonlinear problems. BEM is applied in some cases without the need to mesh all the geometry [47].

In order to make the PDE solvable the boundary conditions should be selected after determining the geometry of the problem. The boundary condition specifies



sufficient information on the boundary to make the solution unique. It describes the effect of any existence fields outside the domain of interest. The choice of boundary conditions can reduce the analysis domain in addition to its influence on the final solution. The main types of boundary conditions are Dirichlet, Neumann condition, Robin and mixed condition [47]. For closed boundary problems Laplace's, Poisson's, Helmholtz's or Fourier's equations may be satisfied. Media existing in region may be linear or nonlinear. All the sources are in the bounded region. But in an open boundary problem Laplace's equation is satisfied. Open boundary problem can be solved by picking an arbitrary boundary far enough from the area of interest [48].

While on the interface between two regions of different electric or magnetic properties inside the domain of interest, interface condition is introduced to connect both sides of the interface [49].

### **1.3 Thesis objectives**

The basic aim of this thesis is to confirm on the existence of eddy current losses in transmission towers under balanced condition, and thesis objective are as follows:

1. Study the influence of low frequency quasi-static magnetic field of transmission lines on the tower holding them.
2. Use the FDM to solve Maxwell's differential equations in low frequency problems.
3. Present a method to estimate eddy current in transmission tower at different material properties under balanced condition.

### **1.4 Significance of this thesis**

This research will present a practical mathematical modeling for estimating eddy current in transmission towers due to low frequency magnetic field of transmission lines under balanced condition. In addition to its importance to researchers interested in the field, this study provides important keys to towers manufacturers in selecting the proper materials so that the eddy-current losses are the slightest.

## **1.5 Arrangement of this thesis**

Chapter 1: this chapter introduces the overview of the topic, giving a summary of previous investigations on transmission lines losses, magnetic field produced by the power lines, the environmental and health effects of power lines' magnetic field.

Chapter 2: a brief descriptions for transmission system is given. Its modeling, losses and efficiency was discussed. Also the losses in the overhead transmission system is presented.

Chapter 3: discusses some theoretical essentials and calculations for the magnetic field in power systems presenting numerical methods that could be used in simulation of the field. Also the theoretical and mathematical formulations of eddy current are discussed. Finally the case of study is introduced and discussed.

Chapter 4: presents the simulation results of the eddy current analysis and power losses due to the eddy current in the transmission tower. Evaluating the results with different metals permeability, conductivity, excitation current, distance and frequency.

Chapter 5: contains the conclusion of the research, and it highlights the future work.

## CHAPTER TWO

### CHALLENGES ASSOCIATED WITH POWER TRANSMISSION

#### 2.1 Modeling of Transmission lines

A transmission line has three constant parameters R, L and C which are distributed along the transmission line. In the equivalent circuit, the resistance and inductance of the transmission line form the series impedance. While the capacitance between a conductor and the neutral of a three phase line or between the two conductors of a single phase line forms the shunt path all over the length of the line. Based on the consideration of the shunt capacitance the overhead transmission lines are classified as short, medium and long length transmission lines [12].

##### 2.1.1 Short transmission lines.

If the length of the transmission line is less than 80km and the line voltage is less than 20kV, the transmission line is defined as a short length-line. In this case, the transmission line can be represented by the single phase equivalent circuit. Assuming balanced conditions, the capacitance is small and hence can be neglected due to the short length of the transmission line and the low voltage level. Therefore, the equivalent circuit of the short length line includes the resistance and inductance as shown in Figure 2.1'.

$$Z = R + jX_L = zl \text{ ohm} \quad 2.1$$

$$zl = rl + jxl \quad 2.2$$

where  $Z$  is the total series impedance per phase,  $z$  is the series impedance of one conductor in ohm per unit length,  $X_L$  is the total inductive reactance of one conductor in ohm,  $x$  is the inductive reactance of one conductor in ohm per unit length,  $l$  is the length of the transmission line.

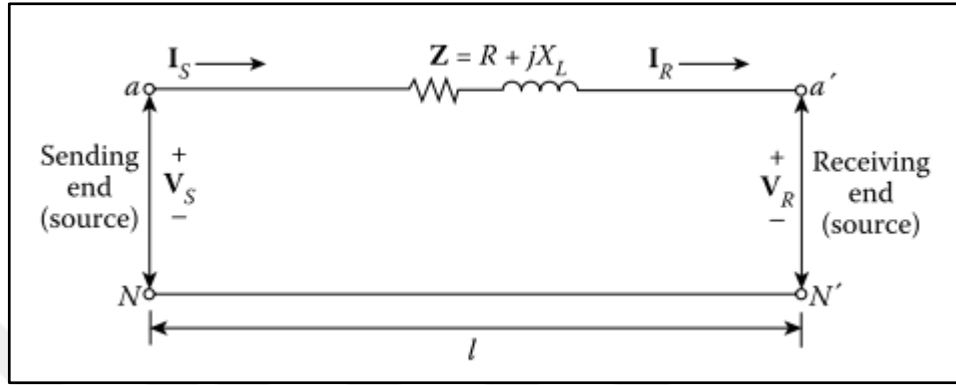


**Figure 2.1:** Equivalent circuit of short transmission line [12].

### 2.1.2 Medium transmission lines.

When the length of the transmission line is about 80 to 240km and the line voltage is between 20 to 100kv, it is defined as a medium-length line. In a medium-length line, the capacitance is taken into account due to the length and voltage level of the line. The equivalent circuit of the medium-length line can be represented in the  $\pi$  or  $T$  configurations as shown in Figure 2.3' and Figure 2.4'.

For the  $T$  circuit in Figure 2.3':

$$V_S = \left(\frac{1}{2}Z\right)I_S + \left(\frac{1}{2}Z\right)I_R + V_R \quad 2.3$$

where  $V_S$  and  $V_R$  are the voltage of the sending and receiving ends respectively,  $Z$  is the series impedance and  $G$  is the shunt admittance.

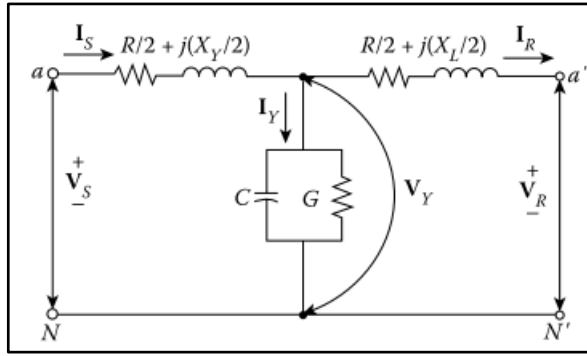


**Figure 2.2:** Equivalent circuit of medium-length line T-circuit [12]

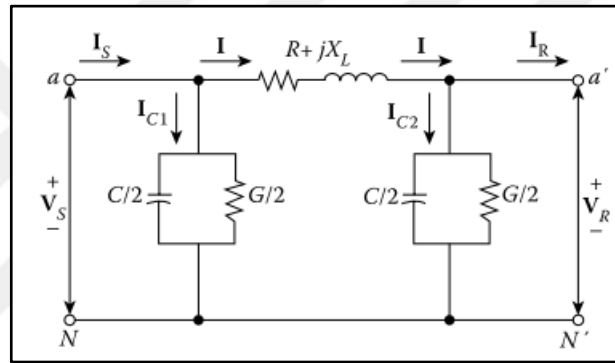


**Figure 2.3:** Equivalent circuit of medium-length line  $\pi$ -circuit [12].

### 2.1.3 Long transmission lines

The transmission line is defined as long-length line when the length of the transmission line is more than 240 km and the line voltage is more than 100kV. Considering the line parameters are uniformly distributed over the whole length of the line. The series impedance and shunt capacitance of the equivalent circuit are calculated by solving the corresponding differential equations, where voltages and currents are defined as a function of time and distance assuming operation conditions of sinusoidal, balanced, steady state conditions with transposed lines. Figure 2.4' shows the equivalent circuit of the long length line with an incremental section  $dx$  at a distance  $x$  from the receiving end, where  $z$  is the impedance per unit length and  $y$  is the admittance per unit length, respectively, The series impedance is  $zdx$ , and the shunt admittance is  $ydx$ .

Then the voltage can be represented as:

$$dV_x = (I_x + dI_x)z dx \quad 2.4$$

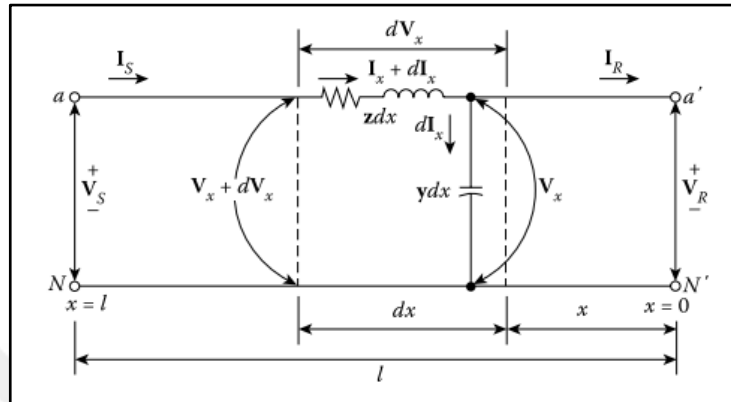


**Figure 2.4:** Equivalent circuit of long-length line [12].

## 2.2 Transmission towers

Transmission towers are complex structures, usually steel lattice towers, supporting the power lines of the overhead power system. They come in different shapes and sizes and are used in AC and DC systems. The typical height of transmission towers are (15-55m). Other materials may be used in addition to steel in the construction of towers, like wood and concrete [8].

### 2.2.1 AC transmission towers

For high voltage and extra high voltage systems, the AC transmission lines of three phase overhead power systems are used. Transmission towers are designed to carry single three phase conductors or multiples of three phase conductors. They are usually made of steel lattices or trusses wooden structures. The insulators are made from glass, porcelain discs or silicone rubber material. They are placed in long rods or strings and their lengths depend on environmental conditions in addition to the line voltage. On top of the tower, two ground wires are placed to divert lightning to the ground.

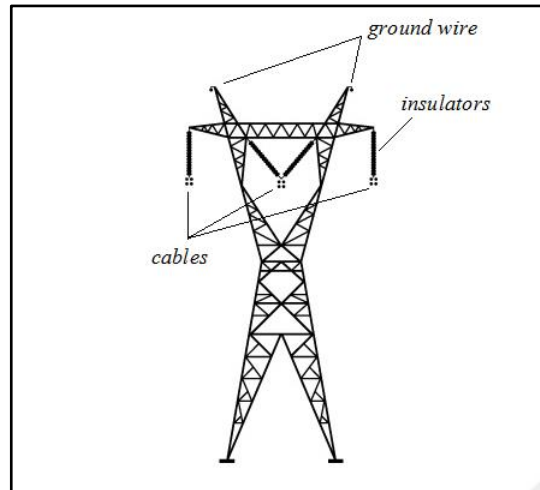


**Figure 2.5:** A typical high voltage AC transmission tower

Towers for high and extra high voltage are usually designed to hold two or more electric circuits. For economic reasons, some transmission towers are designed to carry four circuits but only two or three of them are installed. Also it is common to install different paralleling circuits on the same tower like 110kV, 200kV and 380kV, or carrying railways traction lines in parallel with transmission lines.

### **2.2.2 DC transmission towers**

For long-distance transmission, high voltage DC systems is used because it is less expensive and may have lower electrical losses. It is also used for underwater power lines avoiding the need of large current to charge and discharge the capacitance of cables. High voltage DC transmission lines are from two type monopolar or bipolar systems. In bipolar systems one conductor is carried on each side of the tower. If the ground cable is used as ground return or electrode line, the ground cable must be covered by insulators to avoid the electro-chemical corrosion of the tower. Whereas towers with one conductor can be used for single pole high voltage DC transmission with ground return. Usually when the tower is designed for future conversion plan. In these cases, conductors are installed on both sides of the tower for mechanical reasons. Until the need of the second pole, sometimes it is joined in parallel with the pole in use or used as electrode line. In some high voltage DC transmission lines Electrode line towers are used to hold the power line

between the converter stations to the grounding electrode. These towers are similar to those used for 10–30 kV, however they normally carry one or two conductors.

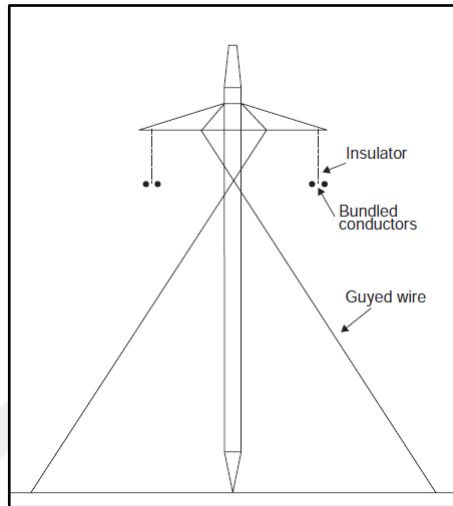


**Figure 2.6:** DC transmission tower.

### 2.2.3 Towers of AC railway traction line

The towers of the single phase AC railway lines are often similar to those used for the three phase 110 kV lines. Traction line towers are made from Steel or concrete. However, the system of railway traction current are single phase two pole AC system, thus suitable towers are designed to hold two cables or multiples of two.

### 2.2.4 Design of towers (transmission and distribution)

A typical tower consists of several parts each of which has a specific function. The peak of tower is the top portion of the tower above the cross arms. Generally, shield wires are connected to the peak of tower. Transmission lines conductors are hold on the cross arms of the tower that installed on the tower cage. The tower cage is the part between the peak and the body of the tower. Cross arm's length depends on the voltage level of the transmission line and minimum forming angle for stress distribution.

There are different classification of towers according to different considerations. One of the classifications depends on the angle of deviation and they are of four type A-type ( $0^{\circ}$  to  $2^{\circ}$ ), B-type ( $2^{\circ}$  to  $15^{\circ}$ ), C-type ( $15^{\circ}$  to  $30^{\circ}$ ), and D-type ( $30^{\circ}$  to  $60^{\circ}$ ). Another



classification is made according to the force that is applied to towers cross arm by conductors to suspension and tension towers. Suspension towers are generally A-type tower, and tension towers include B, C and D-types of tower. Also it can be classified based on numbers of circuits supported by the transmission tower to single, double and multi circuit towers.

#### **2.2.4.1 Suspension towers**

In suspension towers the conductors of the power lines are suspended from the tower, on each side of the tower the mechanical tension are equal. The suspension tower has to hold a lateral and downward forces.

In this case, the tower is supposed to carry a downward force, and a lateral force. Each conductor are connected to the tower via an insulator string which is suspended from the tower, or via two insulator strings as a V-shape. Sometimes several parallel strings are used for higher mechanical strength. These are usually used when a transmission line continues in a straight line, or when it turns through a small angle.

#### **2.2.4.2 Terminal towers**

Terminal towers which are also called anchor pylon are located at end of transmission line, in this type of towers horizontal strain insulators are used at the endpoints of conductors. The endpoints are required when interfacing the mode of the power transmission and when altering the direction of the transmission line. Terminal towers are also located at branch points called branch pylons that are used when the power line runs as overhead and as underground cable.

#### **2.2.4.3 Transposition tower**

Transposition towers are used for transpose the three phase conductors. These type of towers are usually used in long transmission line. The main idea of transposition is changing the three phase arrangement in order to obtain better performance and hence reduce induction and radiation losses in the Transmission line.

## 2.2.5 Materials of transmission towers

Different materials are used in the construction of overhead transmission towers. The selection of the material depends on voltage level, the nature of the area, line model, cost and feasibility of maintenance etc.

### 2.2.5.1 Wooden poles

This type of poles are cheap when compared to other types. Wooden towers are useful for shorter line that spans about 50 m, and suitable for rural areas. The single pole H-shape wooden pole can withstand voltage up to 132 kV. Whereas double pole A-shape or H-shape provide more transverse strength and they are usually used as terminal poles. These supporters are used because they are cheap and considered as natural insulators.

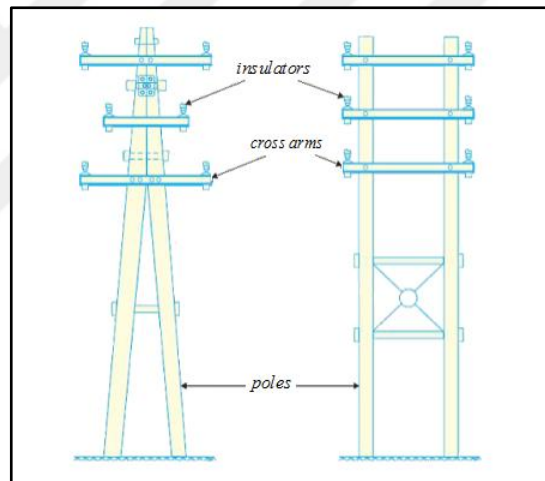


**Figure 2.7:** Wooden pole of A and H-type.

### 2.2.5.2 Reinforced concrete poles RCC

These types of poles are largely used because of their high mechanical strength, they have longer life with low maintaining cost. They also have good insulating property. These pole types are usually used for 33 kV line.

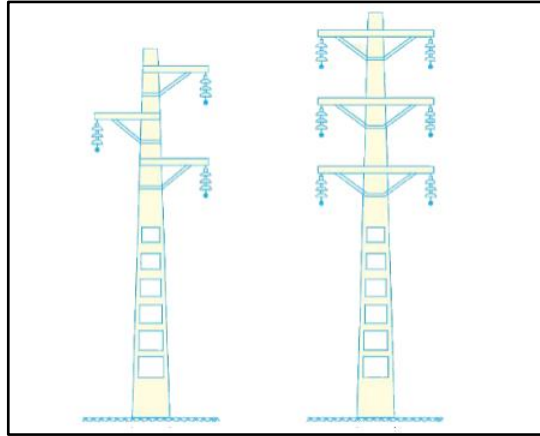


**Figure 2.8:** RCC towers

Reinforced concrete poles are used for longer spans. However the weaknesses points of this type is that they are heavy in weight, thus there are chances of damage during transportation, the high cost of loading and unloading and transportation. To overcome these problems prestressed concrete poles are used which are manufactured at work sites. Also holes are made in poles body to reduce their weight as shown in Figure 2.8’.

### **2.2.5.3 Steel Poles**

Steel poles are used in the distribution system along road sides and inside cities. They are usually used for voltages up to 33 kV, i.e., low and medium voltages. When compared with RCC and Wooden poles, they have higher mechanical strength, lighter weight, and longer life at least 30 years, but they are often costlier. They have to be galvanized periodically to prevent them from corrosion and hence reducing the maintenance cost.

### **2.2.5.4 Steel latticed Tower**

Steel towers are often used for long distance transmission for voltages above 33 kV. Due to longer span, the risk of interrupted service and cost of insulation is reduced to a large level. As the tower footing are grounded breakdowns and lightning problems are also reduced. They are usually made of steel due to its high mechanical strength, long life, and its ability to withstand bad climatic conditions.



**Figure 2.9:** A steel lattice tower

### **2.3 Losses in transmission line**

An overhead transmission line is a very complex electrical system. Its target is to transmit power safely and efficiently from one end (supplier) to the other (consumer). It is composed physically of many components of different materials which have variety electrical and mechanical properties [1]. Like all others, electrical power system, waves around the whole country and it is the largest interconnection of a functional system in presence to date. No matter how accurately this system is designed, losses exist. And including losses due to atmospheric conditions, resistance, theft, miscalculations, etc. That is, the source is supplying power, but is not all reaches the load. The power system is affected by certain losses. These losses affect the energy that should reach the consumer from the energy supplied utility. An essential amount of energy will be lost in the transmission and distribution systems. Many internal and external factors cause this wasteful energy in the power system.

Basically, electrical power system losses can be classified as non-technical losses which are caused by external factors and technical losses those cause by internal factors.

Technical losses in power system are related to the physical properties of power systems component. The wasted power in transmission lines and transformers due to internal electrical resistance is the most obvious example of the technical losses. Technical losses are computable and can be controlled. While non-Technical losses are caused by external factors that Technical losses computation can't be taken into account like unaccounted load conditions and electrical theft. These losses are more difficult to determine because they are often unexpected by the system operators so no recorded information about it exist.

### 2.3.1 Technical losses

Technical losses are related to the physical nature of the equipment like inefficiency of equipment, characteristics and size of the materials used in overhead lines and equipment. In addition, this includes infrastructure of the power systems, i.e., the excitation losses, square current losses through a resistance, and corona or leakage losses in the conductor cables, switches, transformers, and generators.

So technical losses can be calculated based on the natural properties of components in the power system: resistance, reactance, capacitance, voltage, current, and power are routinely calculated by utility companies as a way to specify what components will be added to the systems [17].

There are three types of losses occurs because of the current flowing in the conductor:

1. **Copper losses:** Conductors finite resistance causes  $I^2R$  losses called Copper losses. The copper losses are higher in AC systems because of skin effect, where the flux density is greater at the center of the conductor and current tends to flow more towards the surface, this phenomenon (skin effect) increases the resistance proportionally to the AC signals frequency.
2. **Dielectric losses:** result from the effect of heating on the dielectric material between conductors. This heat is wasted in the surrounding medium causing energy losses.
3. **Induction and radiation losses:** caused by the electric and magnetic fields surrounding conductors. The power that is dissipated in another line or metallic

object due to the linking of the electromagnetic field of the current carrying conductors inducing current in the object, i.e., induction losses. Whereas those unreturned magnetic lines of force to the conductor when the cycle alternates are called radiation losses, these lines of force are radiated to space and result in power losses.

The concern of this study is the alternating magnetic field that accompanied with the alternating currents in transmission lines. The magnetic field consists of concentric circles of magnetic fields lines of force and their center is at the center of the conductor arranging in planes perpendicular to the conductors. Magnetic fields of parallel conductors interacts with each other (causing flux linkage) and inducing voltage and they interact with conductors placed in the vicinity inducing eddy currents.

### **2.3.2 Non-technical losses**

Actions external to the power system causes non-technical losses, mainly related to power theft. By default, the generated energy should equal the energy received at the end consumer. However, in reality, we have to consider the transmission and distribution technical losses. We need information about loads in addition to the power sources for the determination of the expected losses in the power system by load-flow analysis. The difference between supplied energy recorded at a substation must be equal to the consumed energy by the consumers that appears on bills. The difference, if exists, between this actual losses and the expected losses indicates the existence of non-technical losses in the system. Non- technical losses are not easy to measure because they are unaccounted by the system operators. Non-technical losses mainly related to power theft. Theft of power is the energy supplied to customers that is not recorded by the energy meter for the customer. In lower levels distribution networks non-technical losses are more dominant. They include illegal lapping of lines, metering errors, equipment vandalisation, inaccurate valuation of non-metered supplies, inaccuracies of meter reading and inaccurate customer billing.

## 2.4 Transmission efficiency

The obtained power at the receiving end of the transmission line is usually less than the power supplied from the sending end due to losses in the line resistance. This effects the transmission efficiency. So, the efficiency is defined as the ratio of receiving power to the sending power:

$$\eta = \frac{V_R I_R \cos \varphi_R}{V_S I_S \cos \varphi_S} \times 100\% \quad 2.5$$

where  $\eta$  is the transmission efficiency,  $V_R, I_R$  and  $\cos \varphi_R$  are the voltage, current and power factor of the receiving end,  $V_S, I_S$  and  $\cos \varphi_S$  are the voltage, current and power factor of the sending end, respectively.

## CHAPTER THREE

### MAGNETIC FIELD AND PROBLEM DEFINITION

#### 3.1 Magnetic field around transmission lines

Based on Ampere's law whenever a current flows in a conductor, electric and magnetic fields are produced. Electrical power systems include transmission and distribution overhead lines. Electric and magnetic fields are generated by transmission lines. Whereas, in distribution systems weak electric fields are generated but strong magnetic fields can be generated [25]. So transmission lines' alternating currents are always accompanied with electromagnetic fields. An electrostatic field is generated in the vicinity of the overhead line due to the line voltage. In addition, a magnetic field is generated in the vicinity due to the current flowing in the conductors. The intensity of this magnetic field is affected by the magnitude of the current, bus height, phases spacing, distance from the source, phase configurations, lateral distance between towers, and the amount of phase unbalance in terms of magnitude and angle.

The magnetic fields of the overhead lines are represented by concentric circles of field lines surrounding the conductor. The strength of the magnetic field at any point around the conductor is represented by a field vector which is perpendicular to the radius. Figure 3.1' illustrates the magnetic field lines around a current carrying conductor where the direction of the magnetic field is defined based on right hand rule. Recently investigation of transmission lines magnetic field has been one of important concerns because of its effect on human's health and the operation of electric and electronic devices in the vicinity of high voltage transmission line which are very close to the building nowadays. Many methods was presented for the minimization of the harmful magnetic field. Although according to WHO no real prove that magnetic radiation from power



transmission line is harmful to the human being. However, still researchers are concerned about it [25].

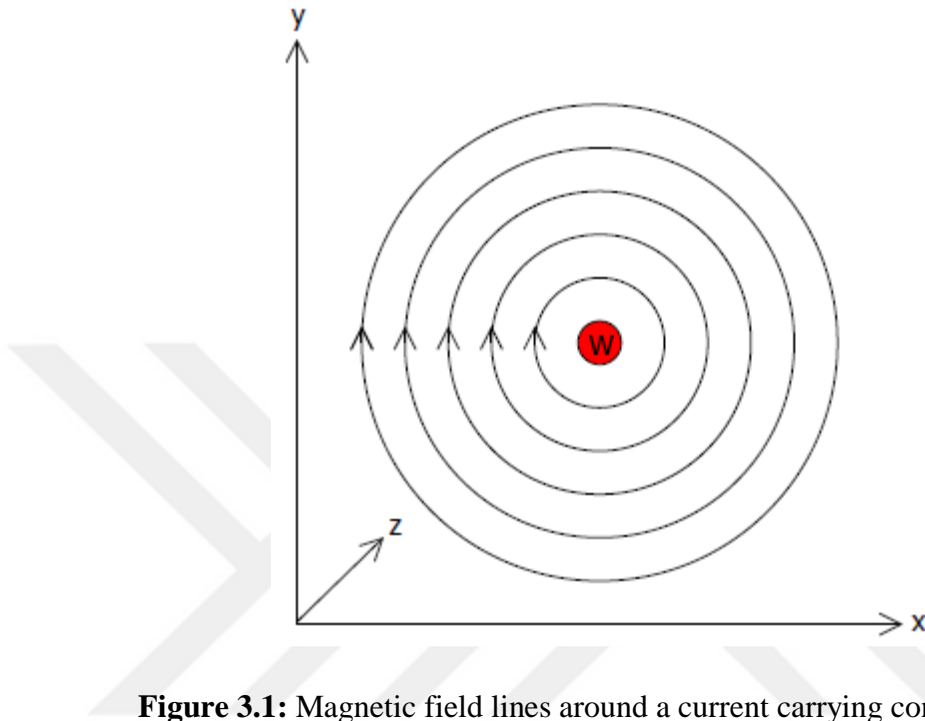


**Figure 3.1:** Magnetic field lines around a current carrying conductor [22]

Our concern here is the interaction of the magnetic field with the transmission tower based on the fact that most transmission towers are made of steel, hence losing energy in term of eddy currents in the steel is noteworthy.

The common laws used for the calculation of magnetic fields is Biot-savart law and Ampere's law.

### **3.1.1 Biot-savart law**

Biot-Savart's law is the most common method used for the calculation of the magnetic field produced around power lines [25]. The Biot-savart law describes the magnetic field by the magnitude and direction of the source current. So it connects the magnetic field to the current source producing it. It is used for the computation of the magnetic field  $B$  generated by a current element  $dl$  that carries a current  $I$  at the point  $p$ .

$$B(p) = \frac{\mu_o}{4\pi} \int \frac{Idl \times r'}{|r'|^3} \quad 3.1$$

where  $(dl)$  is a vector whose its magnitude is the length of the differential element of the wire in the direction of current,  $(r')$  is the displacement vector from the wire element  $(l)$  to the point where the field is computed  $(p)$ .

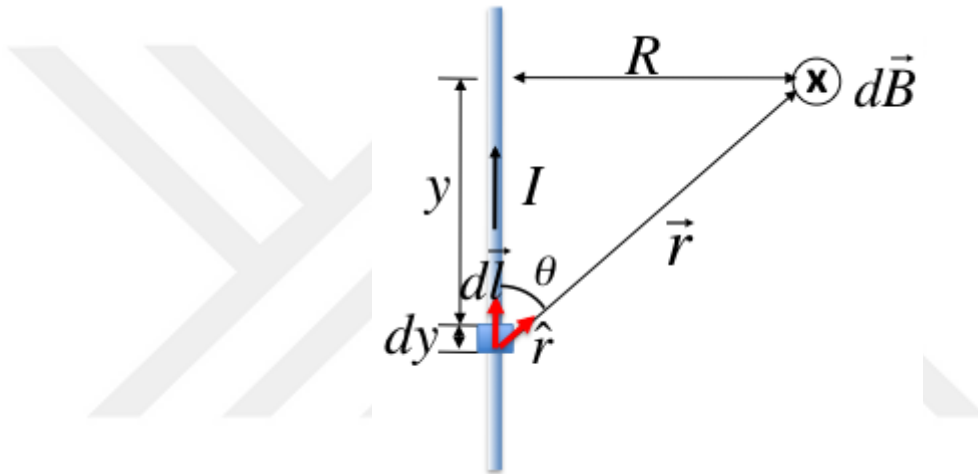


Figure 3.2: Biot-savart law

### 3.1.2 Ampere's Circuital Law

Ampere's law describes the relationship between the current that flowing in a conductor and the magnetic field produced around the conductor, so it is a special case of Biot-savart law. Ampere's Law can be represented in integral or differential form. The integral form of the law states that the circulation magnetic field is equal to the enclosed current.

$$\oint B \cdot dl = I_{enc} \quad 3.2$$

where  $B$  is the magnetic flux density,  $I$  is the current enclosed by the length  $l$

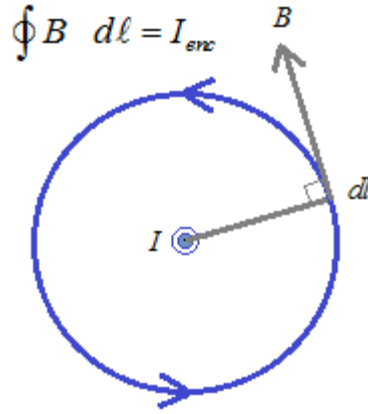


**Figure 3.3:** Ampere circuital law

### 3.2 Eddy current formulation

According to Faraday's law when a magnetic field produced by an alternating current links a conductor a circulating current within the body of the conductor is induced in such a direction that is opposite to the source field due to Lenz's law. The name of eddy current came from the fact that it looks like eddies caused by turbulence of flow in fluids. The eddy current is affected by many factors like frequency of the source current, the position of the conductor from the source, the geometry of the conductor and the conductivity and permeability of the metal [50].

In quasi-static field problems where the frequency is low as in transmission lines. The displacement term is neglected assuming that no flow of currents normal to the surface of the conducting media, and the presence of charges on the surface opposes any tendency for such currents to flow normal to that surface.

$$J_e = j\sigma\omega\vec{A} \quad 3.3$$

$$P_{eddy} = \frac{1}{2\sigma} \iint J_e J_e^* dx dy \quad 3.4$$

where  $A, \omega, \sigma$  are the magnetic vector potential, angular frequency and conductivity respectively.  $p_{eddy}$  is the eddy current losses,  $J_e$  is the eddy current density,  $J_e^*$  indicates the complex conjugate of the eddy current density.

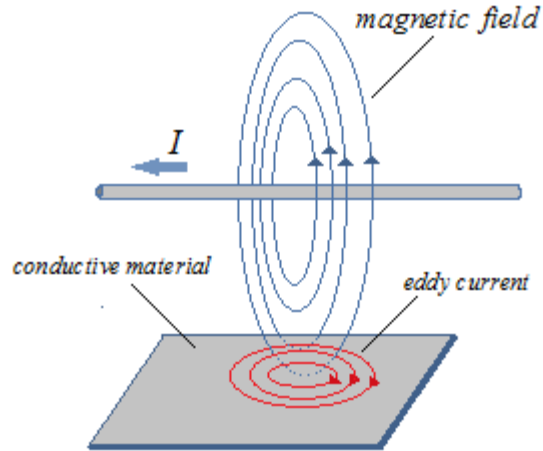


**Figure 3.4:** The induction of eddy currents

### 3.2.1 Faraday's Law

Faraday's Law states that any changing magnetic field will produce a corresponding electric field in the linking conductor thus producing a current in the conductor. Faraday's law is the essential law for understanding the induction of eddy currents. The equation of faraday's law states that the electric field is proportional to the changing magnetic field over time, that is,

$$E = -\frac{\partial B}{\partial t} \quad 3.5$$

where  $E$  is the electric field and  $B$  is the magnetic flux density.

### 3.2.2 Lenz's Law

Lenz's Law describes the direction of electric field on conductors relative to a magnetic field. Generally, Lenz's law states that the induced current in a conductor tends

to oppose the source that induces it thus, in other word induced currents in a conductor will produce a magnetic field that opposes the inducing magnetic field.

### 3.3 Maxwell's equation

Maxwell's equations consist of a set of partial differential equations describes the theoretical foundation for all electromagnetic-field theory. They are Showing the property of the electric and magnetic field and how they propagates, interact, and how they affects and affected by objects in the vicinity. Maxwell's Equations are used to understand and control the behavior of electromagnetic fields. There are two form of the four Maxwell's equations: integral and differential form for every equation:

#### 3.3.1 Gauss's law for electricity

Gauss' law is one of Maxwell's equations used for electric field calculation. It states that the electric flux leaving a surface is equal to the charge enclosed within the surface. The Gauss's law for electricity permits the calculation of the electric field by the symmetric Gaussian surface around a charge distribution and hence calculating the electric flux as:

$$\oint \vec{E} \cdot d\vec{A} = \frac{q}{\epsilon_0} \quad , \quad \nabla \cdot E = \frac{\rho}{\epsilon_0} \quad 3.6$$

where  $(E, q, \rho, \epsilon_0)$  are the electric field, enclosed charge, charge density and permittivity of the free space, respectively.

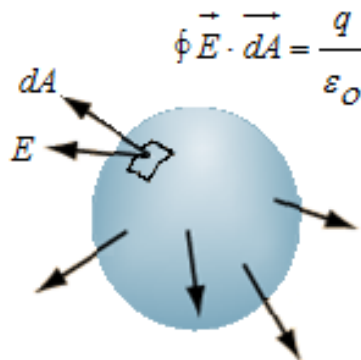


**Figure 3.5:** Gauss's law for electricity

### 3.3.2 Gauss's law for magnetism

The net magnetic flux through a closed surface is equal to zero. This is because the magnetic field consists of continuous loops, so the magnetic lines going in are equal to the magnetic lines going out. Coming up with other laws Gauss's law for magnetism provides the calculation of magnetic field in symmetric cases [51].

$$\oint \vec{B} \cdot d\vec{A} = 0 \quad , \quad \nabla \cdot B = 0 \quad 3.7$$

where B is the magnetic flux density, A is the magnetic vector potential.

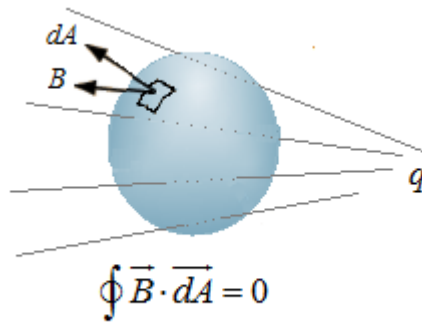


**Figure 3.6:** Gauss's law for magnetism

### 3.3.3 Faraday's law of induction

Faraday's law is the fundamental law of electromagnetism expressing the interaction of the magnetic field and electric circuits producing an electromotive force (EMF), this phenomenon is called electromagnetic induction. So it states that the net electrical field around a closed loop equals the rate of change of magnetic flux in the enclosed loop. Maxwell-faraday equation is one of Maxwell's equations which states that any time varying magnetic field is associated with an electric field and vice versa [52].

$$\oint \vec{E} \cdot d\vec{l} = -\frac{d}{dt} \iint B \cdot ds \quad , \quad \nabla \times E = -\frac{\partial B}{\partial t} \quad 3.8$$

where E is the electric field and B is the magnetic flux density.

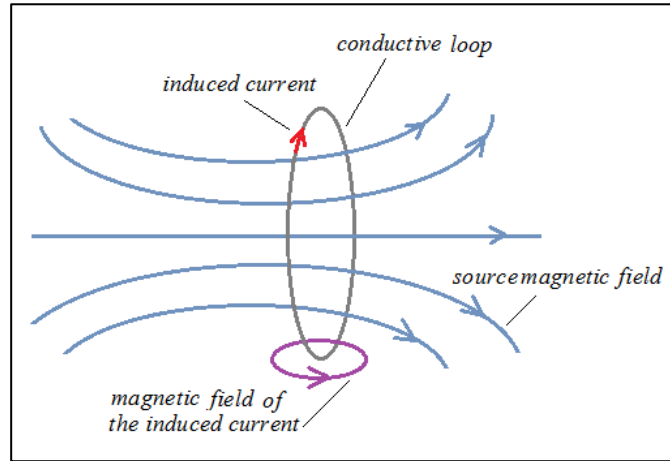


**Figure 3.7:** Faraday's law of induction

### 3.3.4 Maxwell's form of Ampere's circuital law

The Maxwell's form of Ampere's law is used in non-static cases by introducing the displacement current. It states that the line integral of the magnetic field induced around a closed loop is proportional to the electric current plus displacement current.

$$\oint H \cdot d\ell = \iint J \cdot ds + \frac{d}{dt} \iint D \cdot ds \quad , \quad \nabla \times H = (J + \frac{\partial D}{\partial t}) \quad 3.9$$

where H, J, D are the magnetic field intensity, current density and electric displacement field respectively.

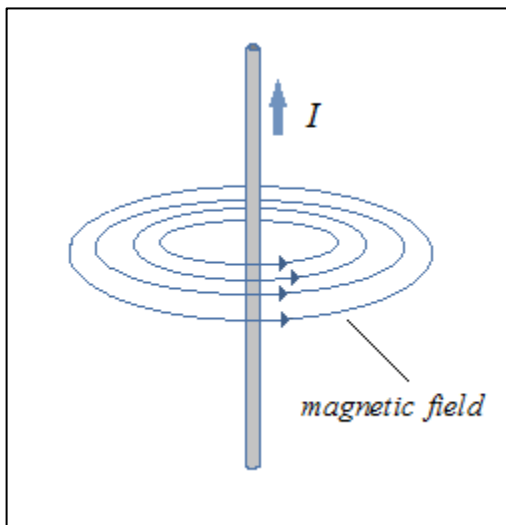


**Figure 3.8:** Ampere's circuital law

### 3.4 Numerical methods

To solve a partial differential equation (PDE) analytically (i.e. exact solution), the PDE should satisfy all boundary and initial conditions associated with the PDE. Most PDEs cannot be solved by exact solution. Thus some numerical approximation must be used [46]. Numerical methods are used for the discretization of the original PDE converting it to a system of linear equations that is solvable and feasible. However, there are some computational error sources while discretizing and solving PDE's [47]:

1. Truncation error: introduced by the finite approximation of an unbounded domain.
2. Round of errors: introduced by the finite approximation of a real number which has infinite digits.
3. Discretization error: introduced when replacing continuous equations by discretized equations.

In the following sections we present the formulation of some common discretization approaches used in electromagnetic problems especially for solving Maxwell's equations:

#### 3.4.1 Finite difference method FDM

The finite difference method is a popular discretization method, due to its simplicity. The FDM provides an efficient technique of solving Maxwell's equations. For electromagnetic problems Maxwell's equations are represented by a system of finite difference equations [53]. According to the fact that most electromagnetic problems are open problems, i.e., the computational domain is unbounded. It's important to use a mesh of limited size large enough to fully contain the problem and in the same time the data can be stored by computers overcoming memory problems. This can be done by putting a boundary condition on the outer surface of the mesh.

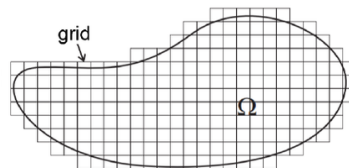


**Figure 3.9:** Discretization of the computational domain by FDM grid



Using five-point stencil finite difference method (FDM) for solving the PDE. FDM approximations of derivatives are obtained by using truncated Taylor series [46]:

$$u(x + \Delta x) = u(x) + \Delta x \cdot \frac{\partial u}{\partial x} + O(\Delta x) \quad 3.10$$

The first order derivative is given by the approximation:

$$\frac{\partial u}{\partial x} \approx \frac{u(x + \Delta x) - u(x - \Delta x)}{2\Delta x} \quad 3.11$$

And the second order derivative is given by:

$$\frac{\partial^2 u}{\partial x^2} \approx \frac{u(x + \Delta x) - 2u(x) + u(x - \Delta x)}{(\Delta x)^2} \quad 3.12$$

where  $u$  is the unknown function and  $\Delta x$  is the width of the finite difference cell, and  $O(\Delta x)$  is the approximation error which is neglected here.

### 3.4.2 Finite element method FEM

Finite element method is also a popular discretization method for solving PDE's. It is a powerful technique especially for electromagnetic problems. FEM is suited to closed domain problems. In open boundary problems approximation should be made [48] like truncation of the external boundary, iterative solution, ballooning, infinite elements etc. FEM uses discretization and interpolation. The computational domain is divided in to small equivalent finite elements each of which is associated to several nodes. The elements have to be chosen to model the actual physical behavior. Every element has its own interpolation function.

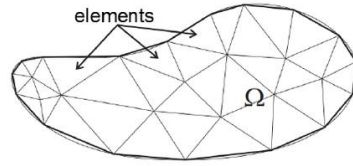


**Figure 3.10:** Finite element method

### 3.4.3 Charge simulation method

Charge simulation method (CSM) describes the electrical potential and field intensity in the form of discrete point charges, ring charges, line charges etc. Their equations derived from electrostatic laws, Coulomb's law and Gauss law. CSM approximates the PDE to a linear combination of fundamental solutions of charges [54].

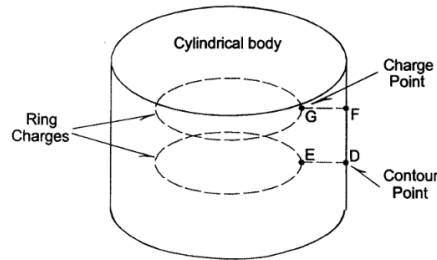


**Figure 3.11:** CSM using ring charges

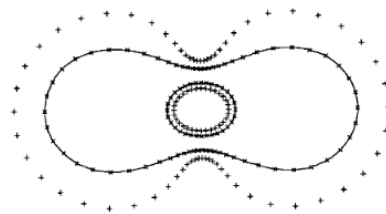


**Figure 3.12:** CSM using point charges

### 3.4.4 Boundary element method

Boundary element method (BEM) is a numerical technique used to discretize integral equations using boundary elements. BEM can be considered as a combination of the finite element methods and the classical boundary integral equation method. In this method the boundary of the computational domain is represented by a set of elements.

The unknowns are approximated by interpolation functions associated with the function at each elements nodes.

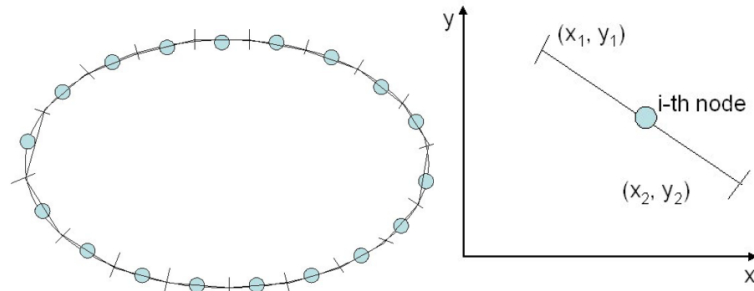


**Figure 3.13:** Discretization of the boundary for BEM [47]

### 3.5 Boundary and interface conditions

The boundary conditions generally can be dirichlet boundary condition where the dependent variable is satisfied along the boundary, Neumann boundary condition where the normal gradient of the dependent variable is satisfied along the boundary, Robin boundary condition, which is the linear combination of dirichlet and Neumann conditions and the Mixed boundary condition where the boundary is divided into two parts applying dirichlet on one part and Neumann on the other [47].

The interface condition for two materials of different permeability [49] can be introduced by applying gauss's theorem:

$$B_{n1} = B_{n2} \quad 3.13$$

where  $n$  denotes the component of the magnetic flux density  $B$  normal to the interface between two regions. For a dielectric interface the component of the electric flux density  $D$  normal to the interface is introduced as:

$$D_{n2} - D_{n1} = q \quad 3.14$$

From ampere's law we can derive another two interface conditions:

$$H_{t1} = H_{t2} \quad 3.15$$

$$H_{n2} - H_{n1} = K \quad 3.16$$

where  $t$  denotes the tangential component of the magnetic field intensity  $H$  and  $K$  is the surface current density on the interface.

### 3.6 Problem formulation

As mentioned before the three phase transmission lines produce electromagnetic field that link the metallic tower and hence, since it is time-varying field, eddy currents are induced in the tower according to faraday's law. Considering that eddy currents flow in relatively small area that is well defined, to minimize the number of unknown variables it is better to define the magnetic field by means of the magnetic vector potential in all regions. Therefore, only one variable (the magnetic potential) is required to be computed by the numerical method.

The following basic assumptions are considered in order to solve for the magnetic field:

1. The phase currents are to be sinusoidal and balanced.
2. Only the  $z$  component of the magnetic vector potential can be observed.
3. Materials have constant magnetic and electric properties and not effected by temperature of surrounding.
4. The field is quasi-stationary field and hence the displacement current is neglected.

As the produced magnetic field by an overhead transmission line spreads in the vicinity as concentric circles of magnetic field. The strength of the magnetic field is inversely proportional to the distance, in other word, the magnetic field gets weaker as you move further from the center of the current carrying wire. This field can be considered as quasi-static field because the transmission line operates at low frequency. The displacement term is neglected assuming that no flow of currents normal to the surface of the conducting media, and the presence of charges on the surface opposes any tendency for such currents to flow normal to that surface. The basic laws of quasi-static field are

Ampere's law with Maxwell addition neglecting the displacement flux density ( $\frac{\partial D}{\partial t} = 0$ ), Maxwell equation of Faradays law, the magnetic flux continuity (Gauss's law for magnetism) and some constitutive relations.

$$\nabla \times \vec{H} = \vec{J}, \quad 3.17$$

$$\nabla \times \vec{E} = -\frac{\partial \vec{B}}{\partial t}, \quad 3.18$$

$$\nabla \cdot \vec{B} = 0, \quad 3.19$$

$$\vec{B} = \mu \vec{H} \text{ and} \quad 3.20$$

$$\vec{J} = \sigma \vec{E} \quad 3.21$$

### 3.6.1 Differential equation derivation

In order to calculate the magnetic field it is common to turn all equations into one equation having one unknown, the magnetic potential field  $\vec{A}$  is introduced by:

$$\vec{B} = \nabla \times \vec{A} \quad 3.22$$

By substituting equation 3.22' in equation 3.18':

$$\nabla \times \vec{E} = -\frac{d\vec{B}}{dt} = -\frac{\partial}{\partial t}(\nabla \times \vec{A}) \quad 3.23$$

$$\vec{E} = -\frac{\partial \vec{A}}{\partial t} \quad 3.24$$

Substituting equation 3.24' in equation 3.21':

$$\vec{J}_e = \sigma \cdot \vec{E} = -\sigma \cdot \frac{\partial \vec{A}}{\partial t} \quad 3.25$$

$$\therefore \vec{B} = \mu \cdot \vec{H} = \nabla \times \vec{A} \quad 3.26$$

Ampere's law:

$$\nabla \times \vec{H} = \vec{J} + \vec{J}_e \quad 3.27$$

By substitution:

$$\nabla \times \left[ \frac{1}{\mu} \cdot \nabla \times \vec{A} \right] = \vec{J} - \sigma \cdot \frac{\partial \vec{A}}{\partial t} \quad 3.28$$

$$\nabla \times \nabla \times \vec{A} = \nabla(\nabla \cdot \vec{A}) - \nabla^2 \vec{A} \quad 3.29$$

Assuming  $(\nabla \cdot \vec{A} = 0)$  Coulomb gauge condition:

$$\nabla^2 \vec{A} - \mu \cdot \sigma \cdot \frac{\partial \vec{A}}{\partial t} = -\mu \cdot \vec{J} \quad 3.30$$

Assuming  $\omega$  is the frequency of a sinusoidal current:

$$\frac{\partial \vec{A}}{\partial t} = j \cdot \omega \cdot \vec{A} \quad 3.31$$

By substituting the formulation of magnetic vector potential to solve eddy current problems this yields:

$$\nabla^2 \vec{A} - j \cdot \omega \cdot \mu \cdot \sigma \cdot \vec{A} = -\mu \cdot \vec{J} \quad 3.32$$

The above Equation 3.32' is the partial differential equation that governs the magnetic field in frequency domain.

To calculate the magnetic field the three phases and the tower was considered as shown in Figure 3.14'. Equation 3.32' can be redefined in every region as follows: in current carrying conductors, equation 3.32' must be satisfied. In the air region  $\Omega_2$ , the equation is reduced to:

$$\nabla^2 \bar{A} = 0 \quad 3.33$$

In the metallic tower  $\Omega_1$ :

$$\nabla^2 \bar{A} - j\omega\mu\sigma \bar{A} = 0 \quad 3.34$$

Open boundary problems can be solved by picking an arbitrary boundary far enough from the area of interest so that either ( $A = 0$ ) for dirichlet boundary condition or ( $\nabla^2 A = 0$ ) for Neumann boundary condition [48]. The distance from the outer boundary to the center of interest should be five times the distance from the outside of the object to the center of interest at least. And because the problem in this study is an open boundary one. The boundary can be defined as homogenous dirichlet boundary conditions ( $A|_{\Gamma} = 0$ ) (see Figure 3.14') placed at large distances from the phases in order to ensure accurate solution.

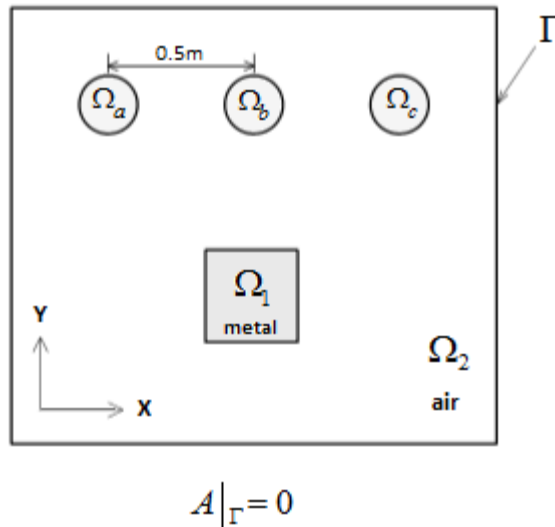


**Figure 3.14:** The geometry of the problem

However, although this approach is widely used for open boundary problems, it needs extra computational resources. To overcome this issue, we reduced the

computational domain to the one shown in Figure 3.16'. That is, the three conductors are excluded from the computational domain and instead the resultant magnetic potential is assigned to the new boundary  $\Gamma'$ . The equation of magnetic vector potential at the outer boundary nodes due to a phase current  $I$  can be calculated as:

$$A = -\frac{\mu_0}{4\pi} \int \frac{J \cdot \vec{r}}{R} \quad 3.35$$

$$A = -\frac{\mu_0}{4\pi} \int \frac{Id\ell \cdot \vec{r}}{R} \quad 3.36$$

$$A = -\frac{\mu_0 I}{2\pi} \ln \frac{r}{R} \quad 3.37$$

$$A_k = -\frac{I_k \mu}{2\pi} \ln \frac{r}{R} a_z, \quad A_p = \sum A_k \quad 3.38$$

where  $A_k$  is the magnetic vector potential due to a conductor of  $R$  radius carrying a current  $I_k$  at the vicinity around the conductor, in other word it is the magnetic field produced by a single phase at a known point,  $\vec{r}$  is the distance vector between a node at point  $P$  to the current carrying conductor,  $A_p$  is magnetic vector potential produced at  $p$  due to three phase conductor.

On the interface between air and the metal, the continuity condition for magnetic field intensity is applied as the interface condition:  $(H_t)_{\Omega_1} = (H_t)_{\Omega_2}$ , where  $H_t$  is the tangential component of the magnetic field intensity [44]. We can derive the equation applied to the interface:

$$H_{t1} = H_{t2} \quad 3.39$$



$$\frac{B_{t1}}{\mu_1} = \frac{B_{t2}}{\mu_2} \quad 3.40$$

$$B = B_x + B_y \quad 3.41$$

$$B_{t1} = B_{t2} \frac{\mu_1}{\mu_2} \quad 3.42$$

$$B = \nabla \times A = \frac{\partial A}{\partial y} a_x - \frac{\partial A}{\partial x} a_y \quad 3.43$$

$$\frac{\partial A}{\partial x} (at x = 0^-) = \frac{\mu_1}{\mu_2} \frac{\partial A}{\partial x} (at x = 0^+) \quad 3.44$$

$$\frac{A_{(x=0^-)} - A_{(x=0)}}{h} = \frac{\mu_1}{\mu_2} \frac{A_{(x=0)} - A_{(x=0^+)}}{h} \quad 3.45$$

$$A_{(x=0^-)} - (1 - \frac{\mu_1}{\mu_2})A_{(x=0)} + \frac{\mu_1}{\mu_2} A_{(x=0^+)} = 0 \quad 3.46$$

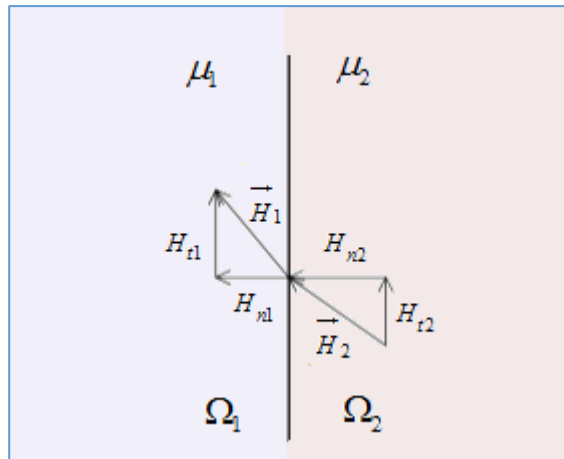


**Figure 3.15:** Interface condition

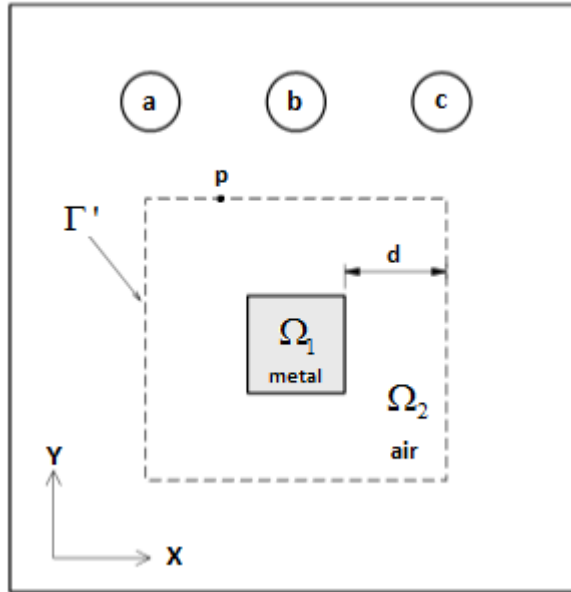


**Figure 3.16:** Reduced computational domain

### 3.7 Problem formulation by FDM

This problem is a two-dimensional problem involving Poisson equation with the consideration that the current density is uniform. For simplification purposes, a square region representing a piece from the tower is considered and the power loss to be computed inside it. At first we define a grid of equally spaced mesh. The geometry was discretized to  $n^2$  nodes,  $(n^2 - 1)$  equal cells of width  $h$  as shown in Figure 3.17' using five-point stencil as represented in Figure 3.18'.

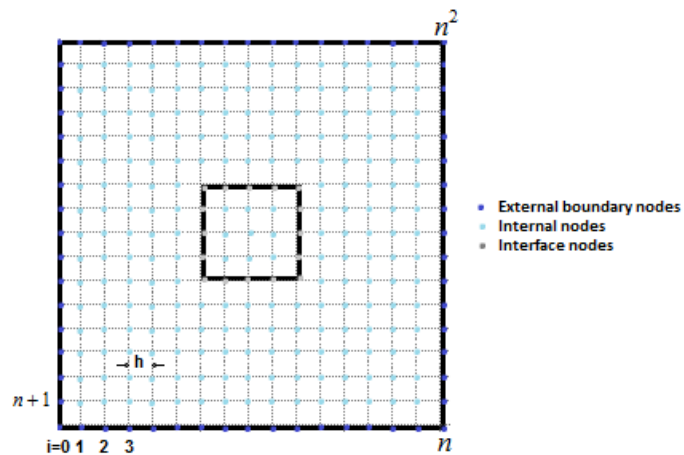


**Figure 3.17:** Problem formulation by FDM

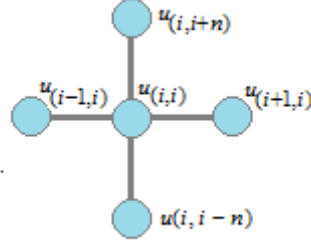


**Figure 3.18:** Five stencil FDM cell

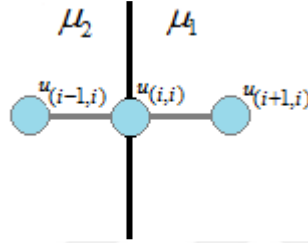


**Figure 3.19:** Interface boundary node

Applying FDM approximations of derivatives equation 3.12' on equations 3.33' and 3.34, to obtain the system of algebraic equations of all interior nodes in  $\Omega_1$  and  $\Omega_2$ :

$$u_{(i+1,i)} + u_{(i-1,i)} + u_{(i,i+n)} + u_{(i,i-n)} - 4u_{(i,i)} - h^2 \beta u_{(i,i)} = 0 \quad 3.47$$

where  $i = 1, 2, \dots, n^2$ ,  $u = [u_1, \dots, u_{n^2}]$  is magnetic vector potential,  $\beta = j\omega\sigma\mu$  and  $h$  indicates the dimensions of the equally spaced cell shown in figure 3.17'.

Applying dirichlet boundary condition at every boundary node from equation 3.38', one can obtain:

$$u_p = -\frac{\mu}{2\pi} (I_a \ln \frac{r_1}{R} + I_b \ln \frac{r_2}{R} + I_c \ln \frac{r_3}{R}) \quad 3.48$$

where  $u_p$  is the magnetic vector potential at any point on the boundary  $\Gamma'$ . On the interface between the metal and the air interface boundary condition is applied:

$$u_{i+1} - (1 - \frac{\mu_1}{\mu_2})u_i + \frac{\mu_1}{\mu_2}u_{i-1} = 0 \quad 3.49$$

## CHAPTER FOUR

### RESULTS AND DISCUSSION

The case study has been modeled and simulated using MATLAB software to calculate the induced eddy current in the tower of the transmission line under balanced condition due to the low frequency quasi-static magnetic field. The following chapter presents and analyzes the simulation and theoretical results implemented to obtain the eddy current in the transmission tower, the geometry of the problem, boundary and interface conditions, magnetic vector potential, eddy current and eddy current losses. Different segments of the tower were considered for the computation of eddy current losses at different places and different metal property.

#### 4.1 Computational domain and boundary conditions

At first a two dimensional geometry of the problem was chosen including cross sections of the three phase line and a piece of the tower as presented in Figure 3.17'. Dirichlet boundary condition is applied on the boundary that truncated at large distances from the phases in order to ensure accurate solution. For the numerical experiment, Figure 4.1' shows the eddy current induced in a random sample of the tower with ( $\mu = 1000\mu_0, \sigma = 10000S/m$ ).

However this is a common technique, it has a disadvantage of needing extra amount of computational resources to make the numerical methods feasible for the calculation of the emitted magnetic fields by power lines in a reasonable time. This consideration justifies the need for new computational domain with new boundary conditions. The problem is redefined according to the fact that the magnetic field at any point in the space can be obtained easily and can be applied as a boundary condition for the new computational domain.

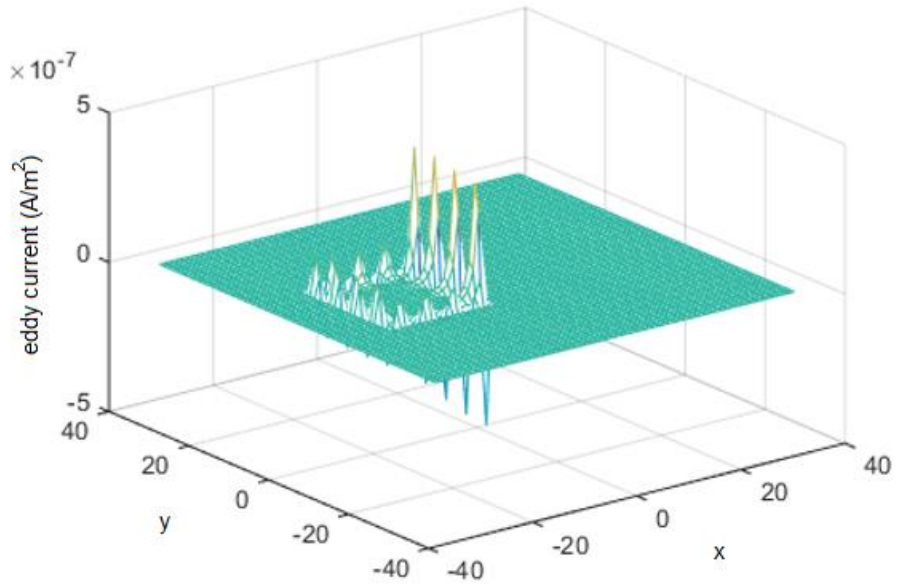


**Figure 4.1:** Eddy current

In order to ensure that the application of the Dirichlet boundary condition is enforced at a distance  $d$  in such a way that it doesn't affect the results, we considered several values of  $d$  and studied where the convergence occurs. Figure 4.2' shows where the convergence occurs, and the error is defined as the difference between two consecutive results evaluated from changing  $d$ . That is, enforcement of Dirichlet condition at  $d=3\text{cm}$  or greater doesn't effect on the solution.

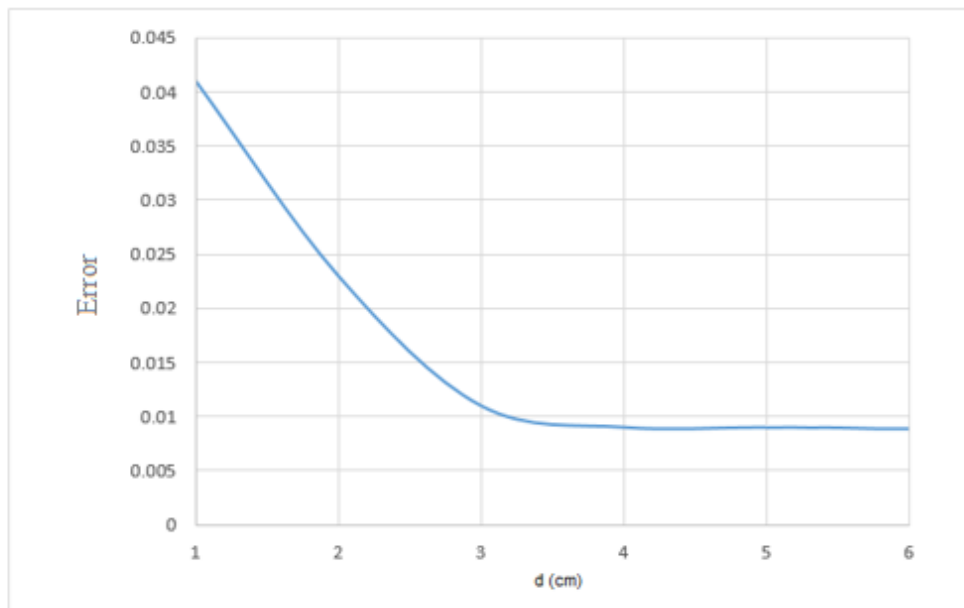


**Figure 4.2:** the impact of  $d$  on the calculation of the eddy current

As shown in Figure 4.3' the influence of the chosen distance  $d$  on the calculated eddy currents at the upper side nodes of the metallic square. From the figure the results for  $d=1$  and  $2\text{cm}$  which are the red and blue curves have different shapes while the results are almost the same for  $d=3,4,$  and  $5\text{cm}$  (green, yellow, and black) respectively.

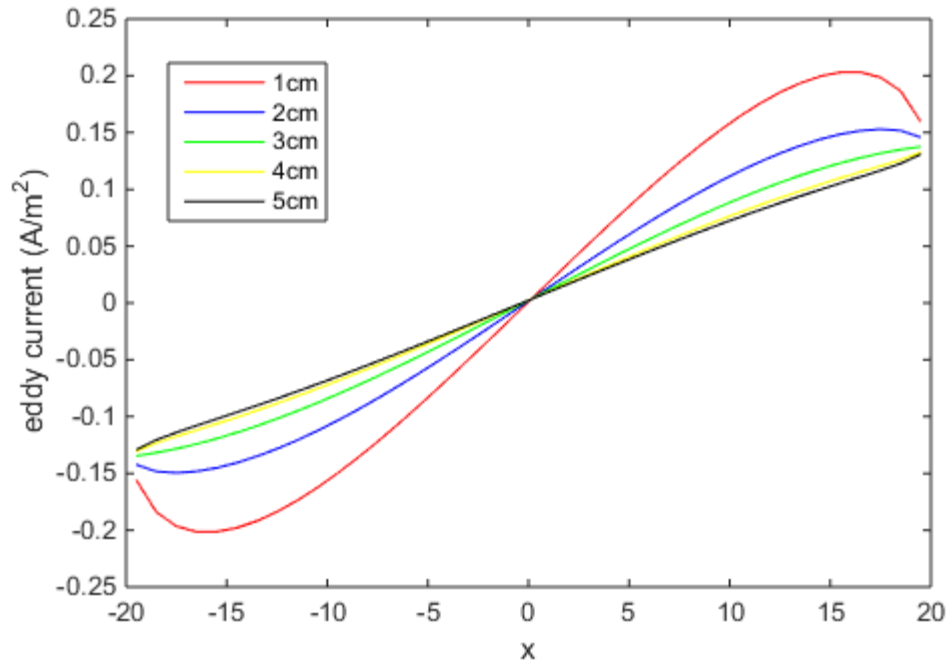


**Figure 4.3:** The influence of  $d$  on the eddy currents in the upper side nodes of the metallic square

## 4.2 Magnetic vector potential

For the calculation of the produced magnetic field Maxwell's equations were solved by finite difference method. This section will present some results evaluated from different samples taken from the tower with different dimensions and properties. The magnetic field of the power line is an alternating field produced by the three alternating phase currents which are changing sinusoidally with time. However it is just the distribution of the magnetic field which changes. For the numerical experiments, the magnetic vector potential is calculated and presented in Figure 4.4' showing the shape of the magnetic vector potential in a  $4\text{cm} \times 4\text{cm}$  metallic segment of the tower with ( $\mu = 200\mu_0, \sigma = 200\text{S/m}$ ) placed at  $1\text{m}$  below the middle phase whose current is  $500\text{A}$ .

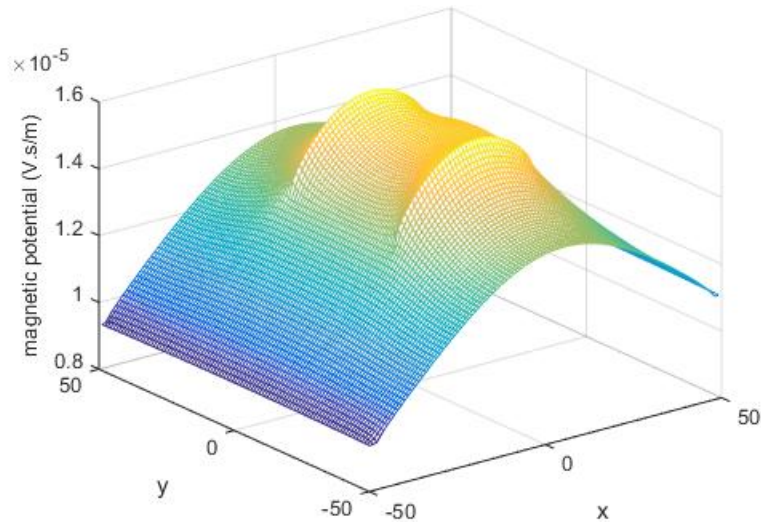


**Figure 4.4:** Magnetic vector potential at  $I=500A$ ,  $\mu = 200\mu_0$ ,  $\sigma = 200S/m$  for maximum current through the middle phase.

Considering different cases the distribution of the magnetic field is changed as presented in Figure 4.5' and 4.6' which illustrate the magnetic vector potential in a  $4cm \times 4cm$  metallic segment of the tower with ( $\mu = 200\mu_0$ ,  $\sigma = 200S/m$ ) placed at  $1m$  below the middle phase whose current is  $500A$ , and where the maximum current is passing through the left phase and right phase, respectively. The distribution of the magnetic field changes with the direction and amount of the currents.

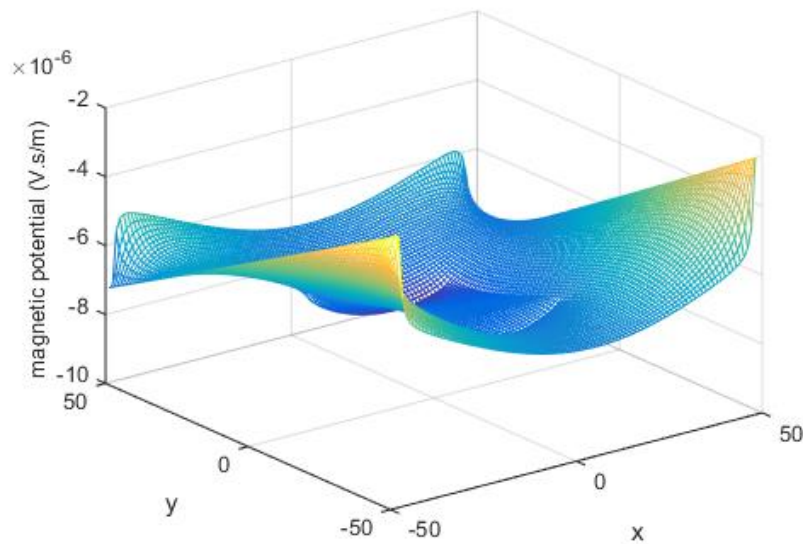


**Figure 4.5** Magnetic vector potential at  $I=500A$ ,  $\mu = 200\mu_0$ ,  $\sigma = 200S/m$  when maximum current passes through the left phase.

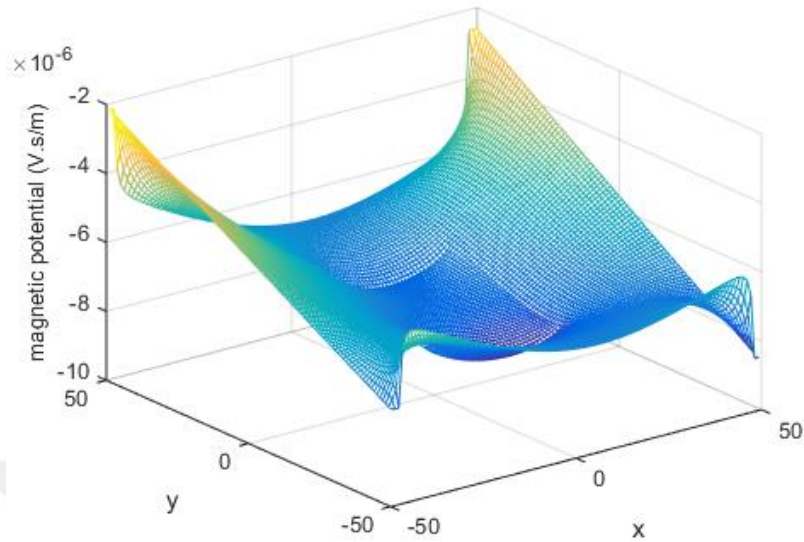


**Figure 4.6** Magnetic vector potential at  $I=500A$ ,  $\mu = 200\mu_0$ ,  $\sigma = 200S/m$  when maximum current passes through the right phase

### 4.3 Eddy current and eddy current losses

Once the magnetic vector potential is estimated, the eddy current that induced in the computational sample of the tower can be calculated according to equation 3.3'. And then equation 3.4' is used to evaluate the associated power losses For the numerical experiments, the eddy currents in a  $4cm \times 4cm$  metallic segment of the tower with ( $\mu = 200\mu_0$ ,  $\sigma = 200S/m$ ) placed at  $1m$  below the middle phase whose current is  $500A$  presented in Figure 4.7', the associated eddy current losses is  $P_e = 0.035W$ .

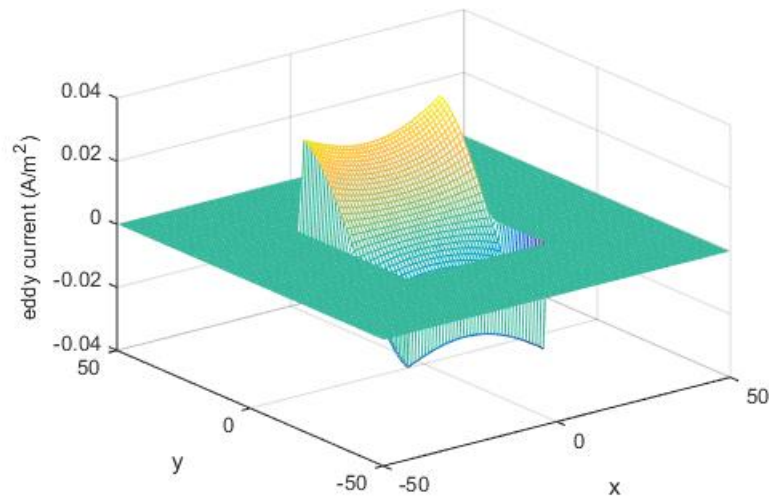


**Figure 4.7** Eddy current at  $I=500A$ ,  $\mu = 200\mu_0$ ,  $\sigma = 200S/m$



The induced eddy current depends on the permeability and conductivity of the transmission tower, dimensions of the computational slice of the tower, the distance to the source, frequency and the excitation current.

### 4.3.1 Permeability of the transmission tower

The permeability of the tower has a dominant influence on the induced eddy currents. The permeability changes effects the distribution of the eddy current. As shown in Figure 4.8' which illustrates the influence of metals permeability on the induced eddy current in a  $(4 \times 4 \text{ cm})$  tower slice.

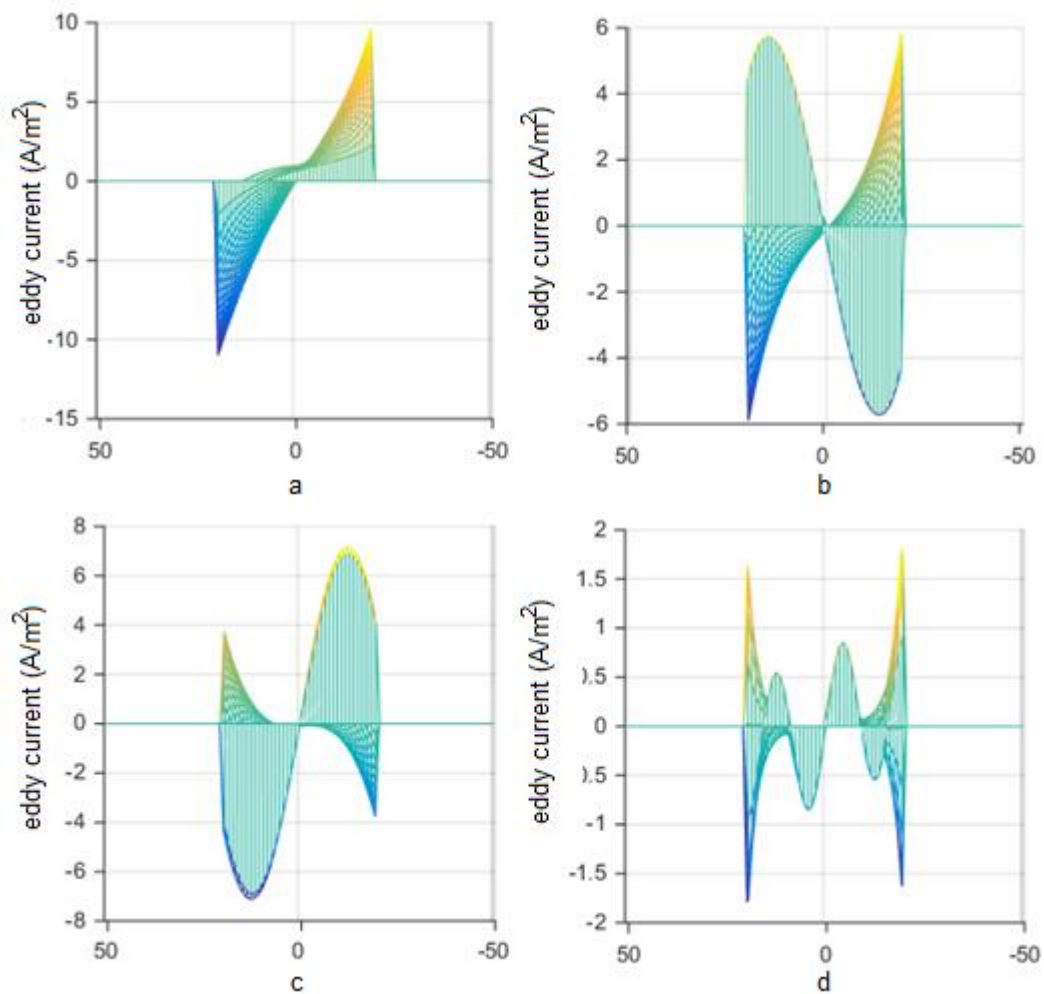


**Figure 4.8** the influence of metals permeability on the induced eddy current. **a)** The eddy current for metal with property of  $(\mu = 30\mu_0)$ . **b)** The eddy current for metal with property of  $(\mu = 20\mu_0)$ . **c)** The eddy current for metal with property of  $(\mu = 15\mu_0)$ , **d)** The eddy current for metal with property of  $(\mu = 5\mu_0)$ .

Figure 4.8.a' shows the eddy current for a metal slice with property of ( $\mu = 30\mu_0, \sigma = 10000S/m$ ) the associated eddy current losses  $P_e = 2.2W$ . However, high magnetic property is not required for the transmission tower thus less permeability used in the simulation of eddy current as indicated in Figure 4.8.b' which shows the eddy currents with ( $\mu = 20\mu_0$ ) that produced losses of  $P_e = 0.23W$ . In Figure 4.8.c' the eddy current losses reduced to  $P_e = 0.16W$  when the permeability reduced to ( $\mu = 15\mu_0$ ). So the less permeability results in less power losses as also shown in Figure 4.8.d' where  $P_e = 0.006W$  with ( $\mu = 5\mu_0$ ). From the estimated results we conclude the influence of permeability on the induced current by the relationship presented in Figure 4.9'.

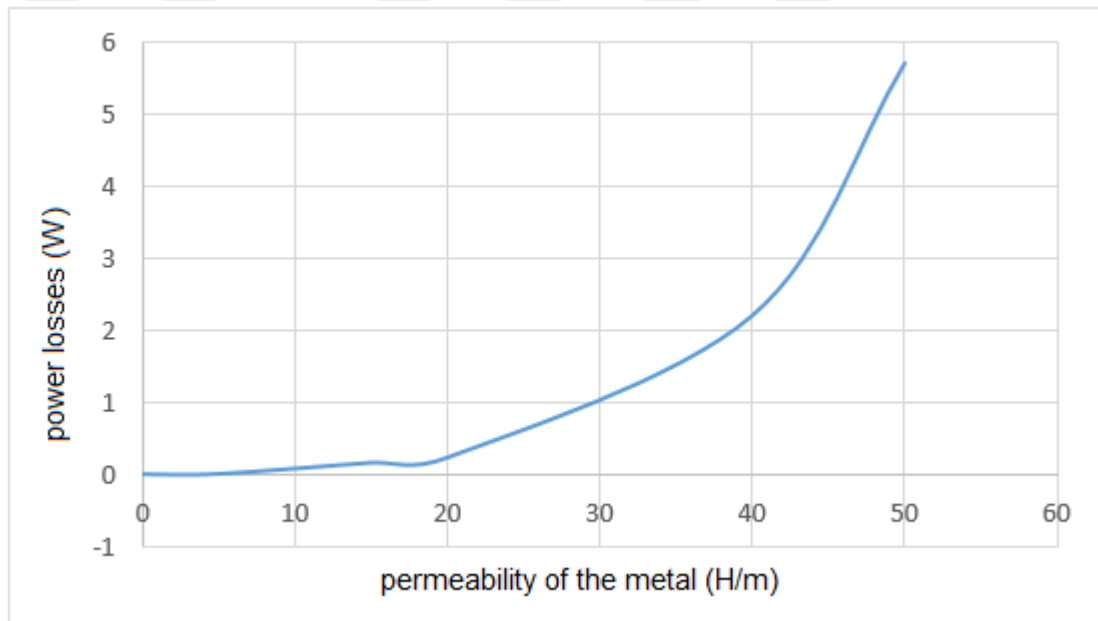


**Figure 4.9:** The relationship between the permeability and the induced eddy current

### 4.3.2 The distance to the source current

As the distance of the computational part to the excitation current increases, the magnetic field reduces hence less eddy current will be induced in the metal resulting in less power losses. These facts are indicated in Figure 4.10' for a  $4cm \times 4cm$  metallic segment of the tower with ( $\mu = 5\mu_0, \sigma = 10000S/m, I = 500A$ ). Figure 4.10.a' illustrates the eddy current for a metal segment 0.5m from the power line and the calculated power loss is  $P_e = 0.05W$ . When increasing the distance to the source to 0.8m

the power losses is decreasing to  $P_e = 0.012W$  as shown in Figure 4.10.b'. Whereas Figure 4.10.c' illustrates the eddy current at a distance of 1m from the source current and the estimated eddy current losses is found to be  $P_e = 0.006W$ . By increasing the distance to 1.5m as calculated in Figure 4.10.d' where  $P_e = 0.001W$ . These results are represented in Figure 4.11' illustrating the relationship between the eddy current induced in the tower and the distance to the source.

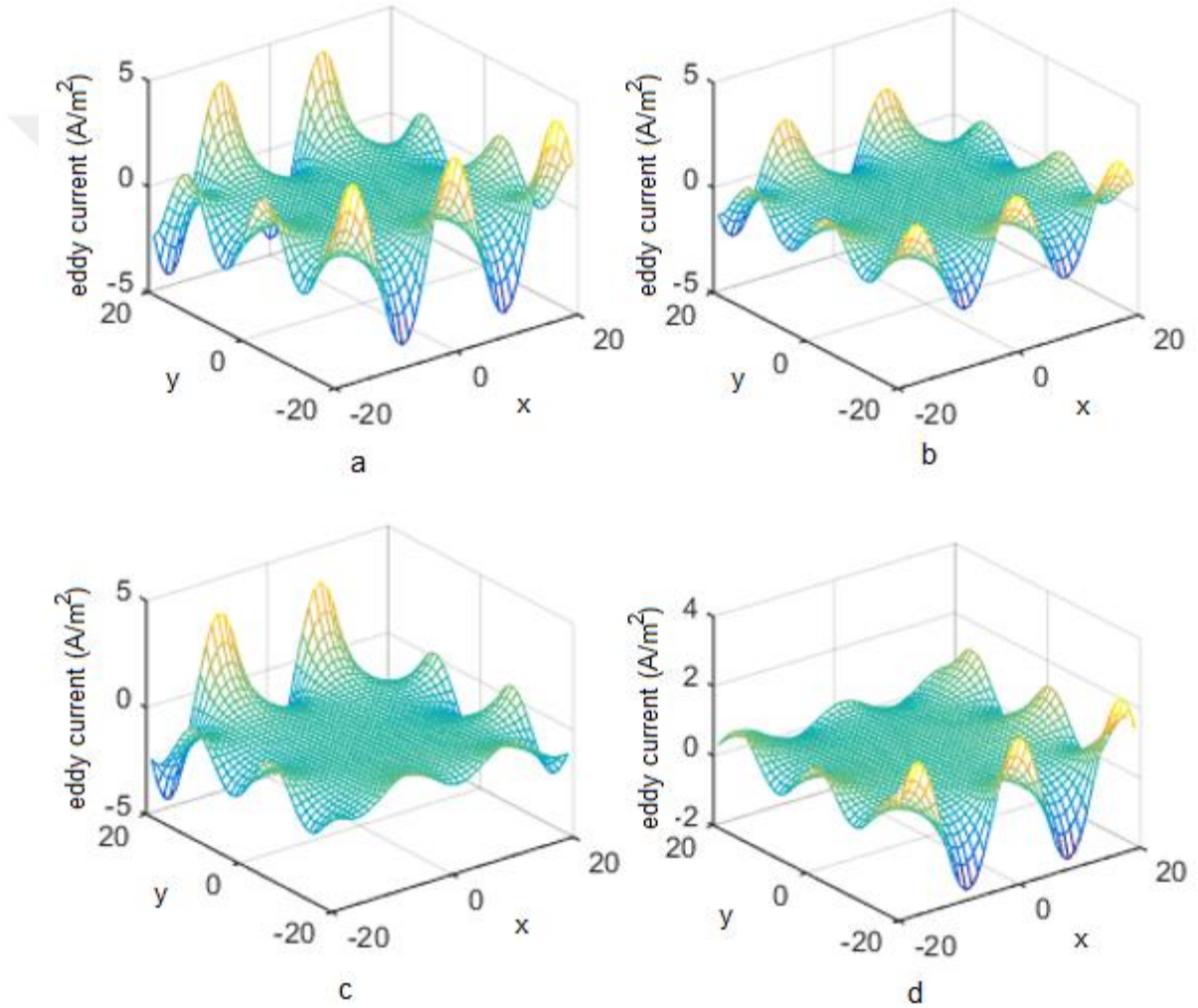


**Figure 4.10** Eddy currents at different distances from the source for with ( $\mu = 5\mu_0, \sigma = 10000S/m, I = 500A$ ): a) 0.5m. b) 0.8m c) 1m. d) 1.5m.

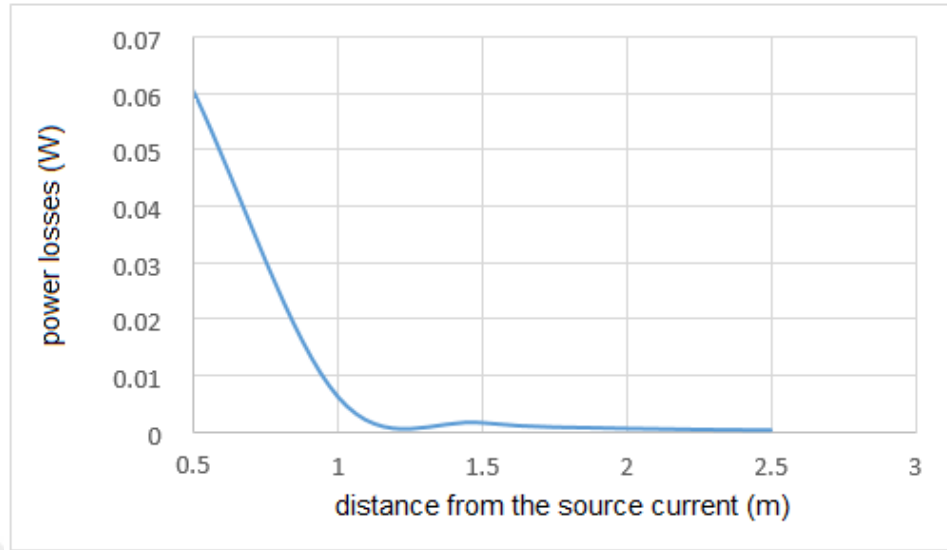


**Figure 4.11:** The relationship between the eddy current and the distance from the source

To see the variance clearly we made the same simulation with changing the permeability and conductivity set to ( $\mu = 200\mu_0, \sigma = 200S/m$ ) that presented in Figure 4.12'.

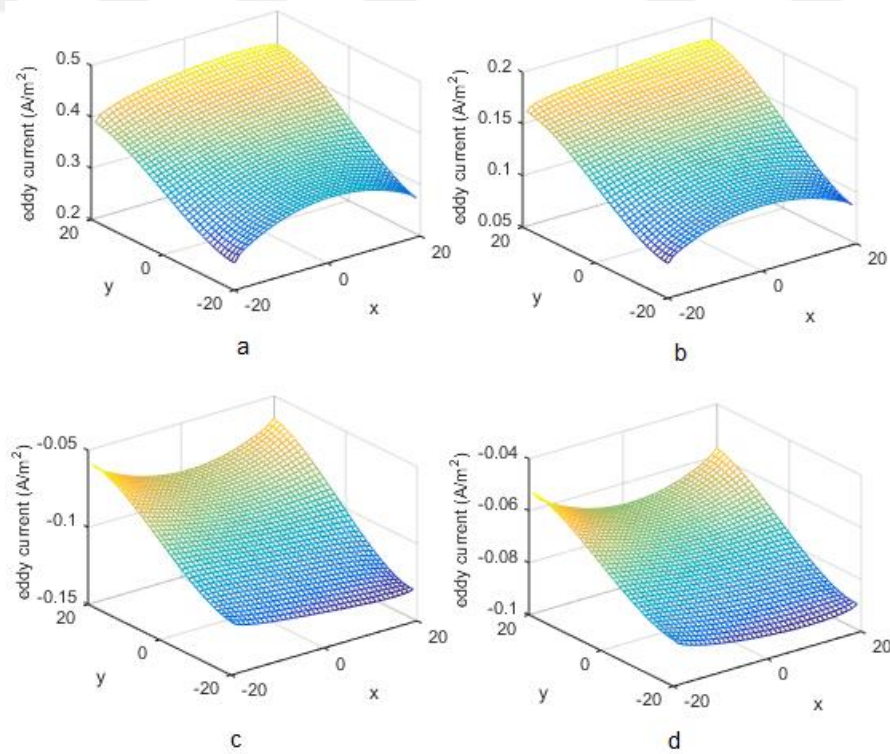


**Figure 4.12:** Eddy current at different distance from the source for with ( $\mu = 5\mu_0, \sigma = 10000S/m, I = 500A$ ): a) 0.5m. b) 0.8m c) 1m. d) 1.5m.

### 4.3.3 Conductivity of the transmission tower

The eddy current induced in the metallic tower also depends on the conductivity of the transmission tower. To see the effect of the conductivity we fixed the permeability of the metal to ( $\mu = 5\mu_0$ ) and the conductivity is changed ( $\sigma = 100, 500, 1000$  and  $10000S/m$  respectively) as indicated in Figure 4.13'. The distribution of the eddy current is not changing while the amplitude is increasing with increasing the conductivity of the metal. The calculated eddy current losses increase from ( $P_e = 6.5 \times 10^{-5}W$ ) for eddy current of the Figure 4.13.a' with ( $\sigma = 100S/m$ ). The losses increase to ( $P_e = 3.2 \times 10^{-4}W$ ) when the conductivity is increased from 100 to  $500S/m$  as shown in Figure 4.13.b'. In Figure 4.13.c' the eddy current tested at ( $\sigma = 1000S/m$ ), and the losses increased to ( $P_e = 6.5 \times 10^{-4}W$ ). While in Figure 4.13.d' the estimated eddy current losses is ( $P_e = 6.5 \times 10^{-2}W$ ) for metal conductivity of ( $\sigma = 10000S/m$ ).

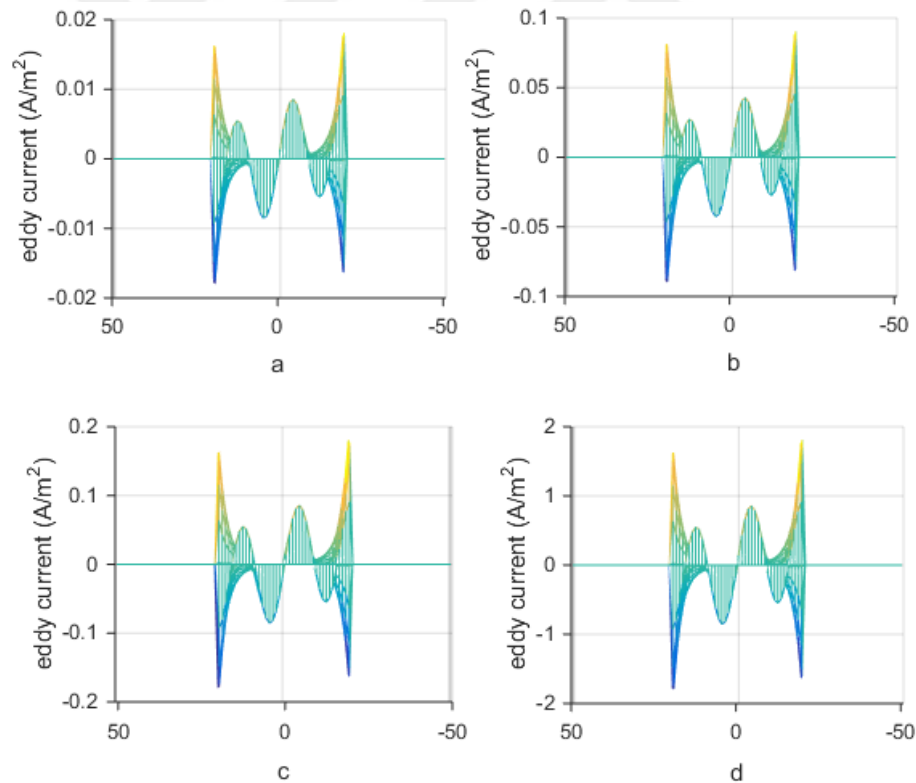


**Figure 4.13:** The influence of metals conductivity on the induced eddy current. **a)** The eddy current for metal with property of ( $\sigma = 100S/m$ ). **b)** The eddy current for metal with property of ( $\sigma = 500S/m$ ). **c)** The eddy current for metal with property of ( $\sigma = 1000S/m$ ), **d)** The eddy current for metal with property of ( $\sigma = 10000S/m$ ).

From the above results it is clear that the relationship between the eddy current and the conductivity of the metal is linear as indicated in Figure 4.14', that is higher conductivity results in higher eddy current losses.

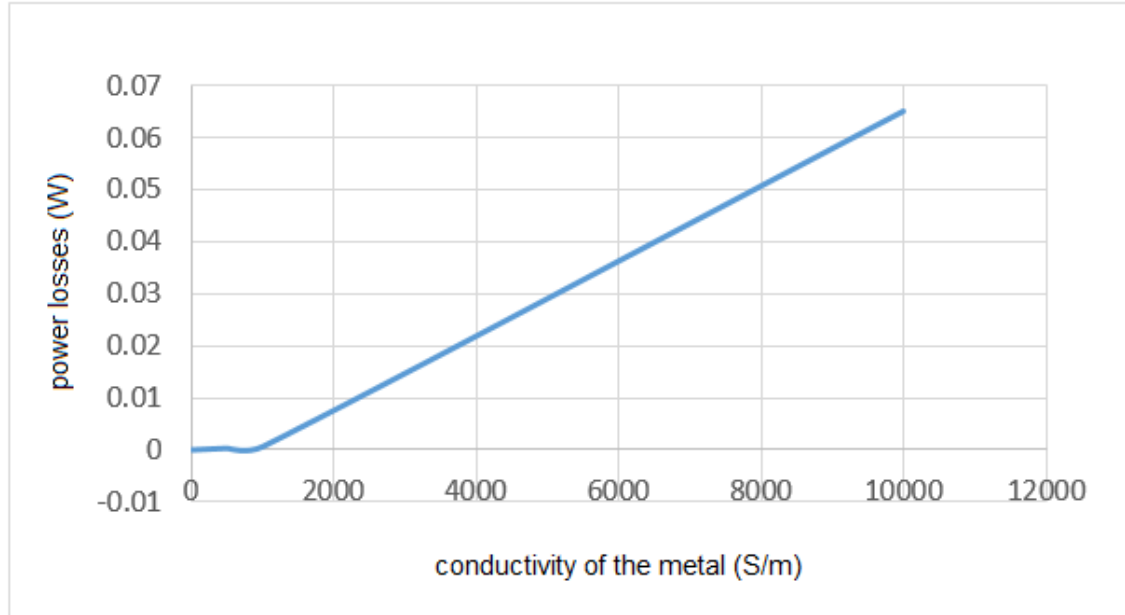


**Figure 4.14:** The relationship between the eddy current and metal conductivity.

#### 4.3.4 Dimensions of the computed area

One of the factors effecting the induced eddy current in a metal is the dimensions and geometry of the metal, however because of the limited computation resources we fixed the geometry of the computational part to a rectangle area. Whereas we can evaluate the results at different dimensions as presented in Figures 4.15', 4.16' and 4.17' for a metal with ( $\mu = 5\mu_0, \sigma = 10000S/m, I = 500A$ ). Figure 4.15' illustrates the eddy current for a metal segment of dimensions ( $2cm \times 2cm$ ) the estimated eddy current losses ( $P_e = 0.0059W$ ). If we used a segment with dimensions of ( $3cm \times 3cm$ ) as in Figure 4.16' the eddy current losses increases to ( $P_e = 0.007W$ ). Figure 4.17' indicates the eddy current induced in a ( $4cm \times 4cm$ ) the associated losses were ( $P_e = 0.0064W$ ).

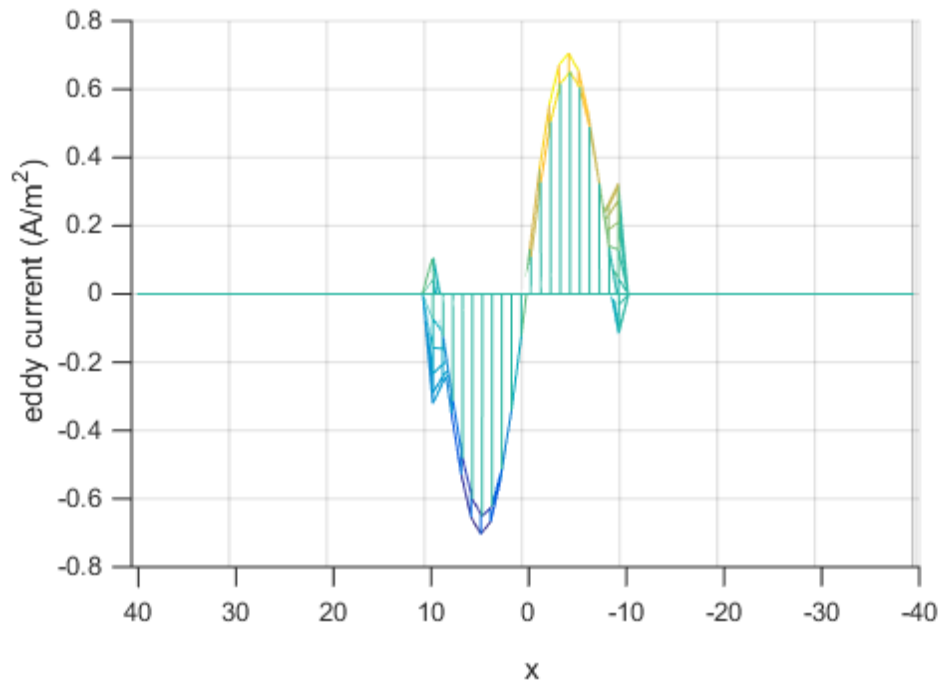


**Figure 4.15:** Eddy current for  $2\text{cm} \times 2\text{cm}$  with  $(\mu = 5\mu_0, \sigma = 10000\text{S/m}, I = 500\text{A})$

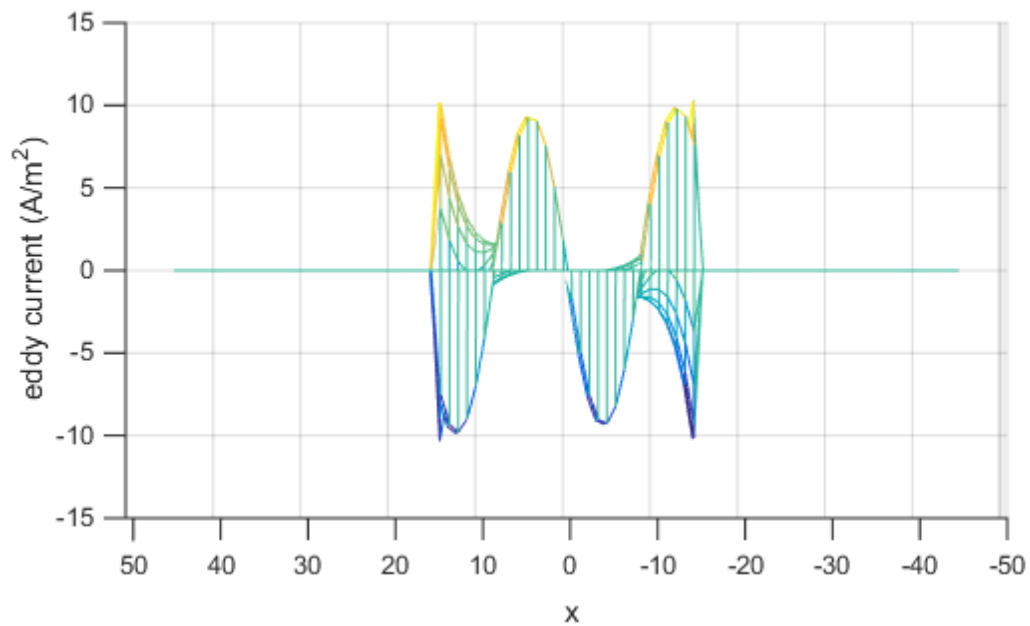


**Figure 4.16:** Eddy current for  $3\text{cm} \times 3\text{cm}$  with  $(\mu = 5\mu_0, \sigma = 10000\text{S/m}, I = 500\text{A})$

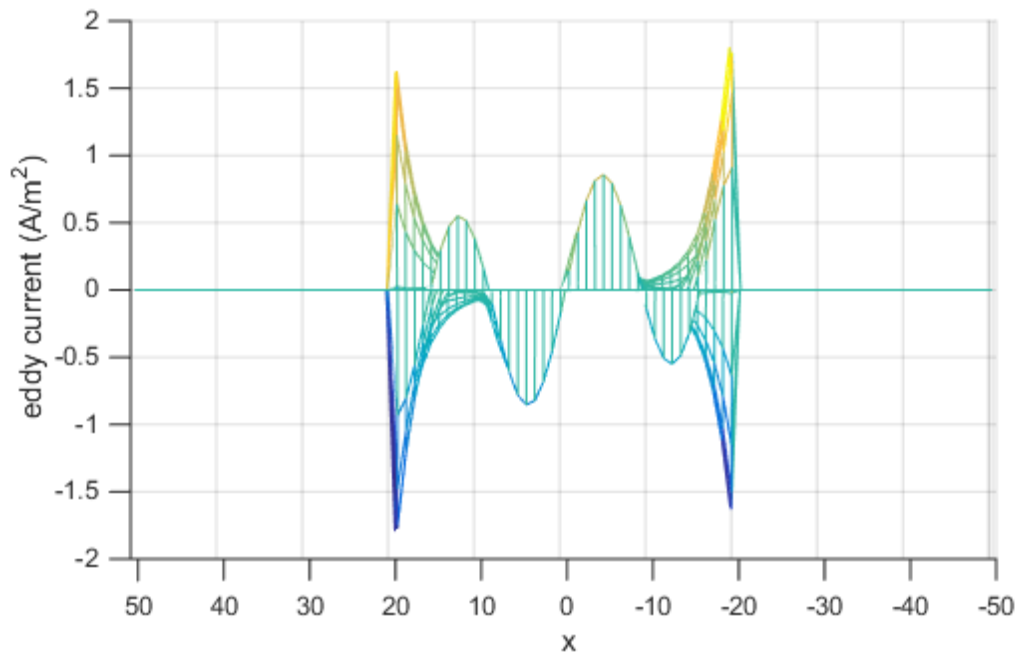


**Figure 4.17:** Eddy current for  $4\text{cm} \times 4\text{cm}$  with  $(\mu = 5\mu_0, \sigma = 10000\text{S/m}, I = 500\text{A})$

### 4.3.5 Excitation current

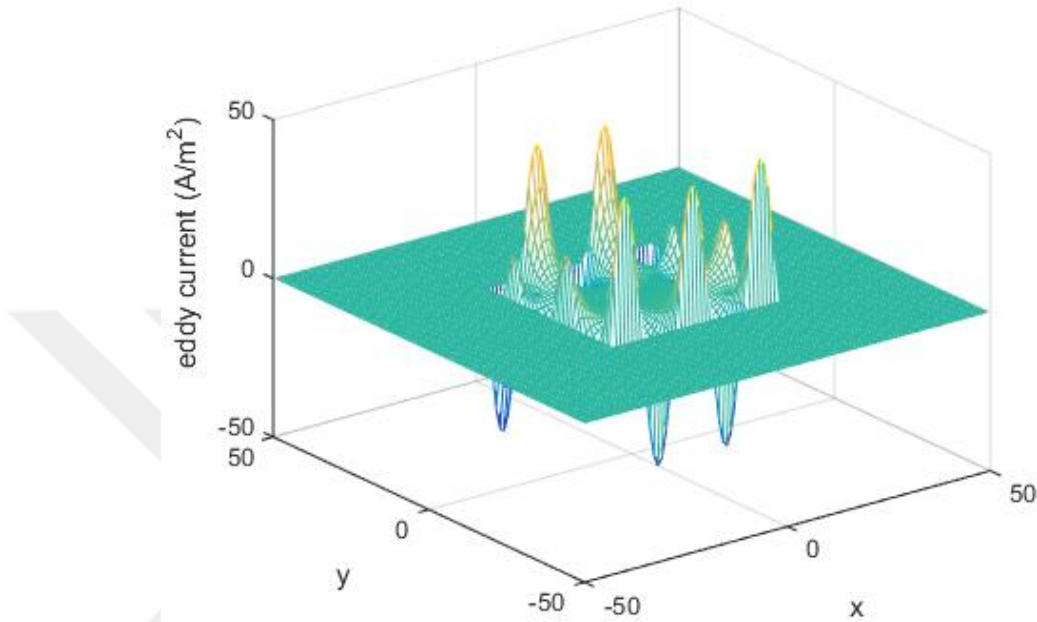
The magnetic field that induces eddy currents in the tower of the transmission line is produced due to the current of the power line. And different transmission lines have different currents carried by different towers having different cross arms with different lengths. Figure 4.18' illustrates the eddy current induced in a  $4\text{cm} \times 4\text{cm}$  metal with  $(\mu = 5\mu_0, \sigma = 10000\text{S/m})$  and the excitation current ( $I = 10000\text{A}$ ) when the distance between each two neighbor phases is equal to  $1\text{m}$  the power losses found to be  $(P_e = 25.7\text{W})$ .

The same simulation have been done this time with less distance  $0.5\text{m}$  between conductors of the power line for Eddy current at  $4\text{cm} \times 4\text{cm}$  with  $(\mu = 5\mu_0, \sigma = 10000\text{S/m}, I = 10000\text{A})$  that is shown in Figure 4.19' where the calculated power losses decreases to  $(P_e = 2.58\text{W})$ .

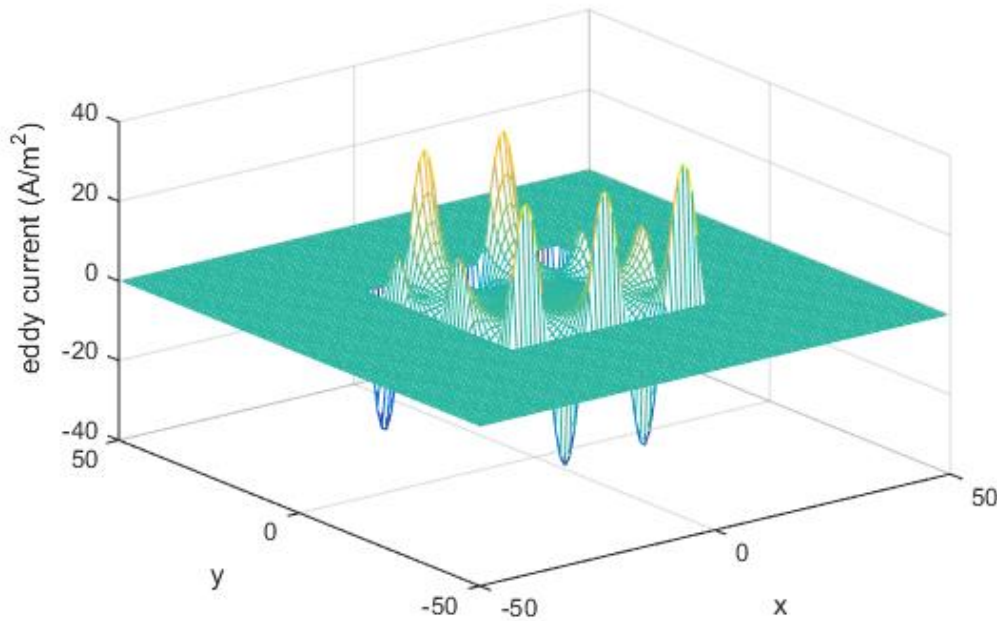
When testing the eddy current at different excitation current, Figure 4.20' shows the eddy current induced in a  $4\text{cm} \times 4\text{cm}$  metal with  $(\mu = 5\mu_0, \sigma = 10000\text{S/m})$  and the excitation current ( $I = 1000\text{A}$ ) when the distance between each two neighbor phases is



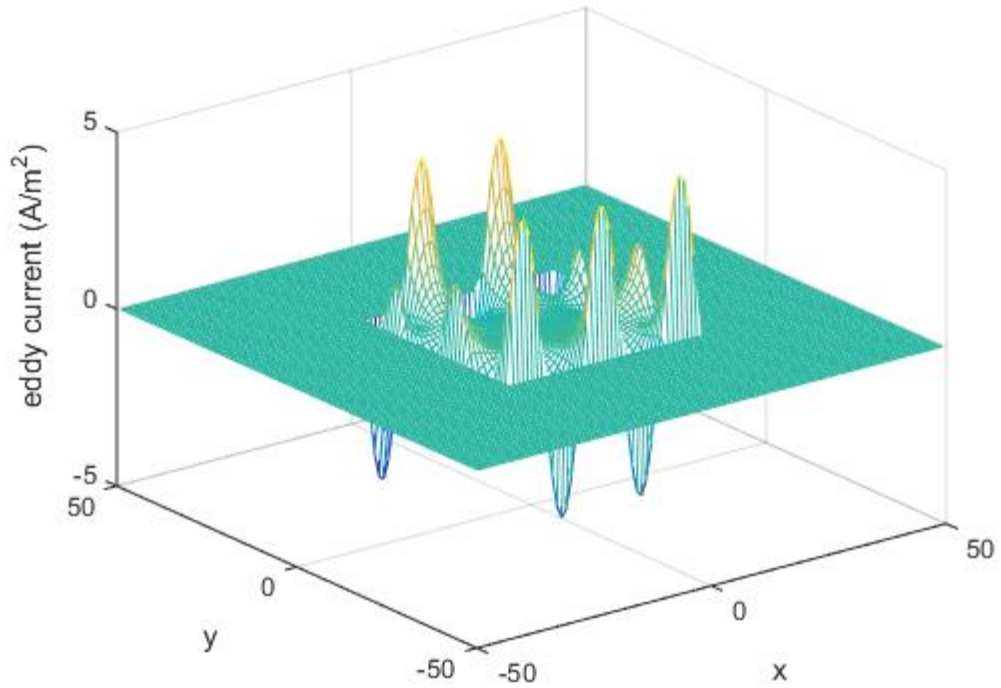
equal to 1m, the corresponding power losses is found to be  $P_e = 2.58W$  which is reduced to ( $P_e = 0.25W$ ) when reducing the distance between the phases to the half 0.5m as in Figure 4.21’.



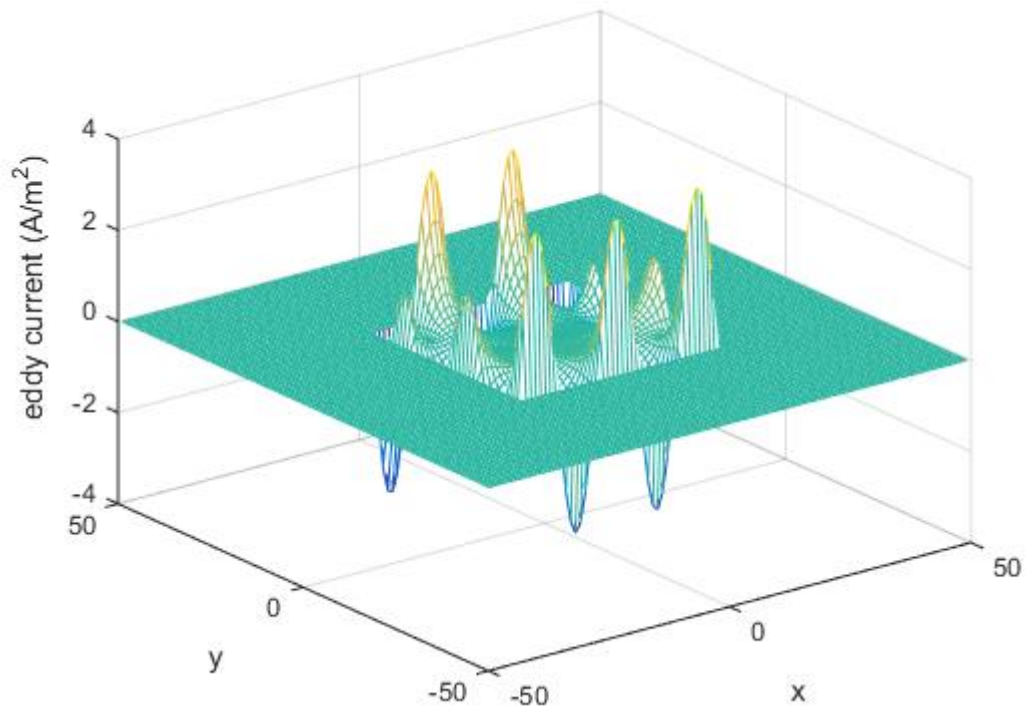
**Figure 4.18:** Eddy current for  $4cm \times 4cm$  with ( $\mu = 5\mu_0, \sigma = 10000S/m, I = 10000A$ ) when the distance between phases is 1m.



**Figure 4.19:** Eddy current for  $4cm \times 4cm$  with ( $\mu = 5\mu_0, \sigma = 10000S/m, I = 10000A$ ) when the distance between phases is 0.5m.

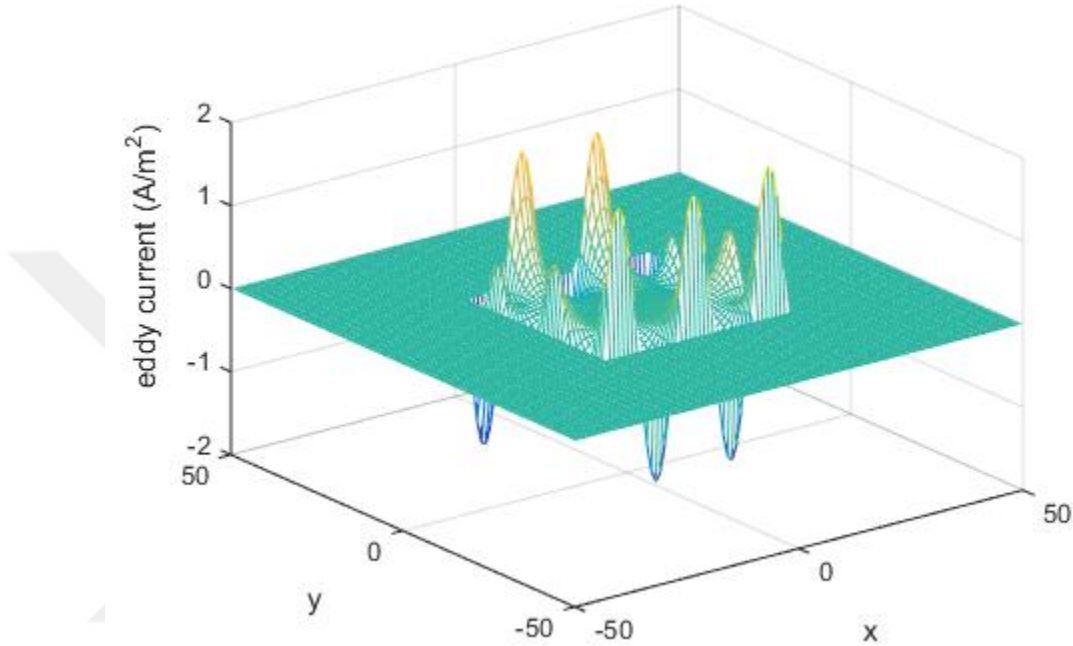


**Figure 4.20:** Eddy current for  $4\text{cm} \times 4\text{cm}$  with  $(\mu = 5\mu_0, \sigma = 10000\text{S/m}, I = 1000\text{A})$  when the distance between phases is 1m.



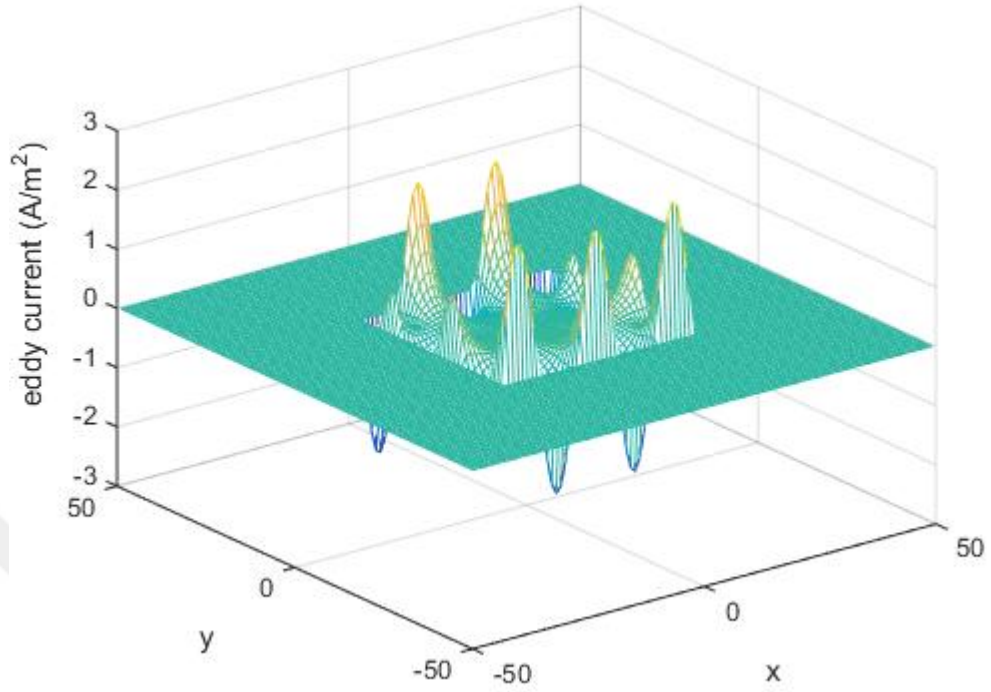
**Figure 4.21:** Eddy current for  $4\text{cm} \times 4\text{cm}$  with  $(\mu = 5\mu_0, \sigma = 10000\text{S/m}, I = 1000\text{A})$  when the distance between phases is 0.5m.

Figure 4.22' clarifies the eddy current at a  $4\text{cm} \times 4\text{cm}$  metal having ( $\mu = 5\mu_0, \sigma = 10000\text{S/m}$ ) with excitation current ( $I = 500\text{A}$ ) at a distance between each two neighbor phases is equal to  $0.5\text{m}$  the power losses found to be ( $P_e = 0.0064\text{W}$ ).



**Figure 4.22:** Eddy current for  $4\text{cm} \times 4\text{cm}$  with ( $\mu = 5\mu_0, \sigma = 10000\text{S/m}, I = 500\text{A}$ ) when the distance between phases is  $0.5\text{m}$ .

For longer cross arm with the same parameters the same simulation have been done with a larger distance of  $1\text{m}$  between conductors of the power line for  $4\text{cm} \times 4\text{cm}$  with ( $\mu = 5\mu_0, \sigma = 10000\text{S/m}, I = 500\text{A}$ ) that is shown in Figure 4.23' where the calculated power losses increased to ( $P_e = 0.064\text{W}$ ). The evaluated results show that the losses is inversely proportional to the length of the cross arm, while it is a well-known fact and best proved by the applied simulations that the losses produced by the eddy current in the transmission tower is linearly proportional to the source current of the power line as indicated in Figure 4.24'.



**Figure 4.23:** Eddy current with ( $\mu = 5\mu_0, \sigma = 10000S/m, I = 500A$ ) when the distance between phases is 1m.

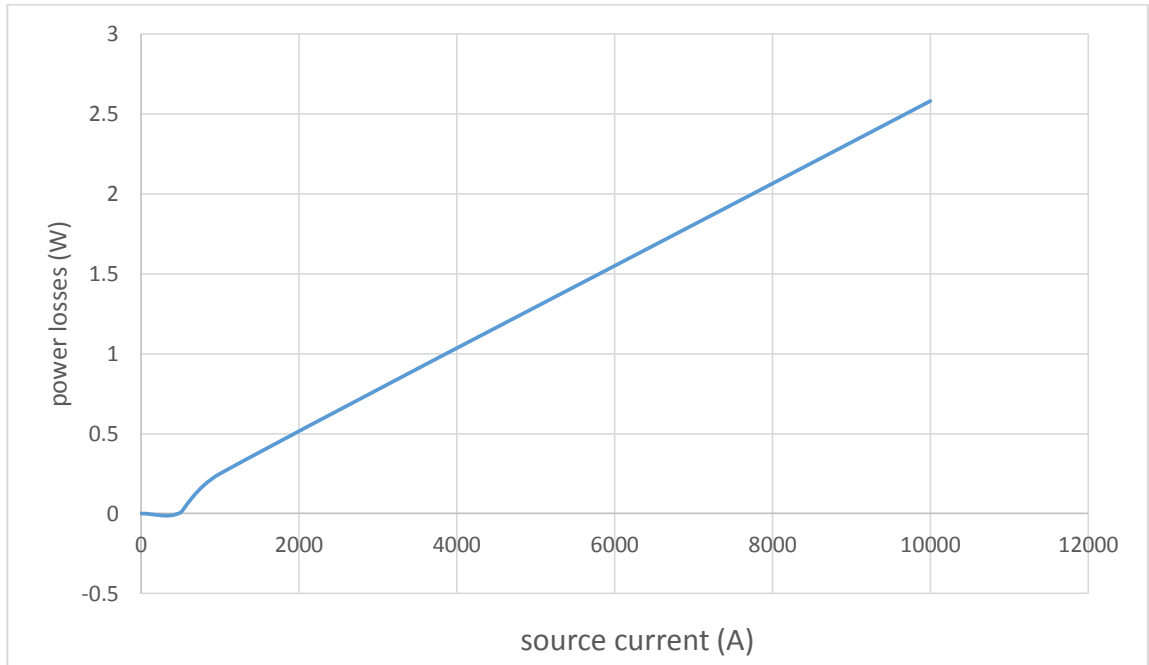


**Figure 4.24:** The relationship between the eddy current and the excitation current

### 4.3.6 Maximum current

The three phase AC transmission line consists of three conductor carrying three sinusoidal currents ( $I_a, I_b, I_c$ ). The three currents have the same amplitude with a phase shift of  $120^\circ$ . At balance condition the summation of them must be equal to zero. So, when obtaining the simulation at different cases it is noticed that only the distribution of the magnetic field which changes and hence the distribution of the eddy current will differ. While the obtained eddy current losses is not affected. Figure 4.25' illustrates the eddy current in a tower slice with ( $\mu = 5\mu_0, \sigma = 10000S/m$ ) and the peak current ( $I_p = 500A$ ). The calculation assumed the instant when the maximum current passes through the middle phase ( $I_b = I_p$ ). The produced losses for this case is ( $P_e = 0.646 \times 10^{-2}W$ ).

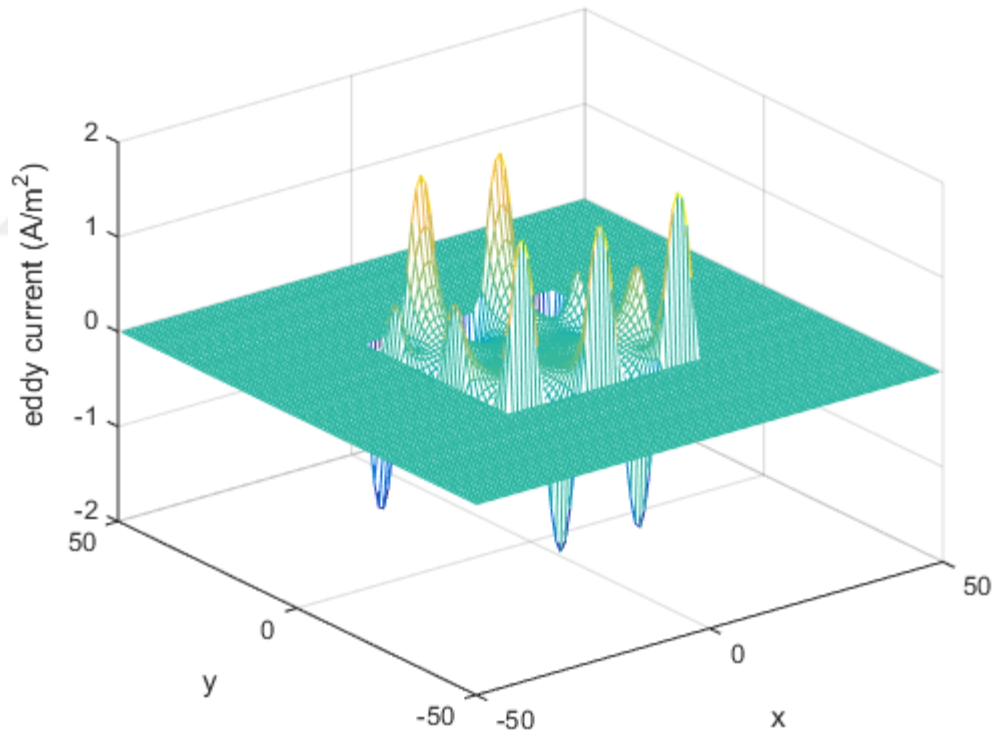


**Figure 4.25:** Eddy current in the metal with ( $\mu = 5\mu_0, \sigma = 10000S/m$ ) considering the instant that a maximum current of 500A passes through the middle phase.

Now considering the instant that the maximum current passing through the left phase is ( $I_b = I_p = 500A$ ), the eddy current in a segment of ( $4cm \times 4cm$ ) the property of the metal ( $\mu = 5\mu_0, \sigma = 10000S/m$ ) is as obtained in Figure 4.26'. The produced

losses is quite the same as the previous case which is ( $P_e = 0.646 \times 10^{-2}W$ ) while the distribution of the eddy current changes.

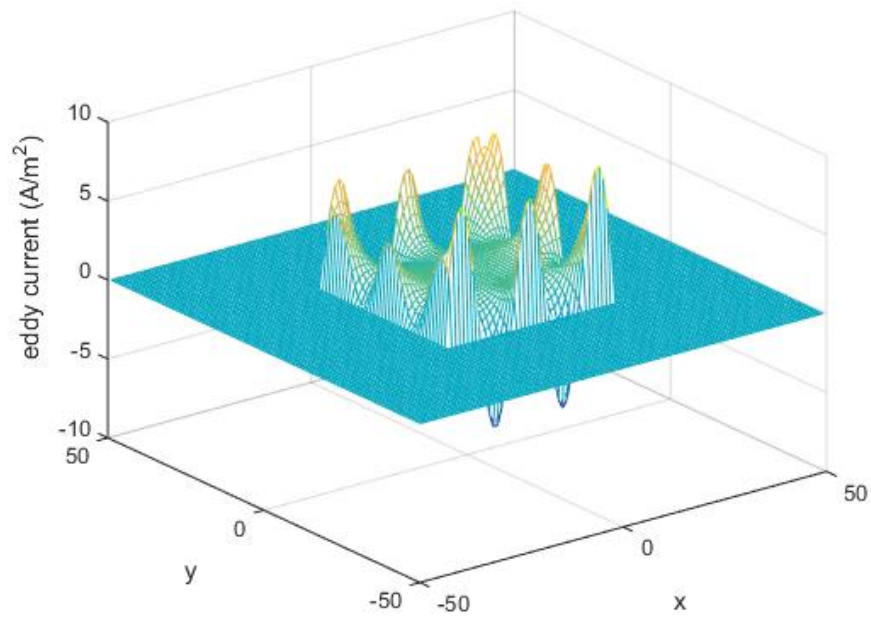


**Figure 4.26:** Eddy current in the metal with ( $\mu = 5\mu_0, \sigma = 10000S/m$ ) considering the instant that a maximum current of 500A passes through the left phase.

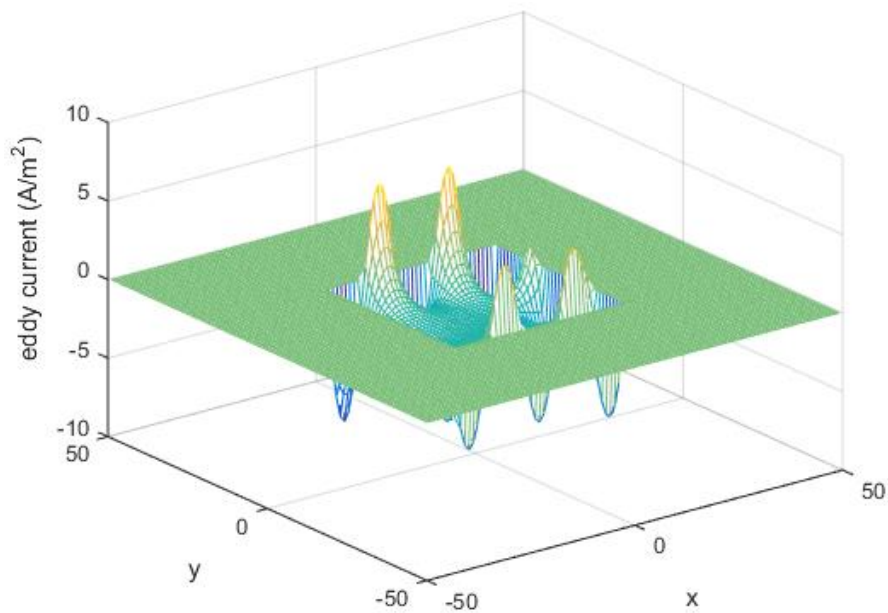


**Figure 4.27:** Eddy current in the metal with ( $\mu = 5\mu_0, \sigma = 10000S/m$ ) considering the instant that a maximum current of 500A passes through the right phase.

In Figure 4.27' the eddy current induced in the ( $4\text{cm} \times 4\text{cm}$ ) metal slice was presented when the maximum current passes through the right phase of the three phase line ( $I_c = I_p = 500\text{A}$ ). The estimated power losses is ( $P_e = 0.646 \times 10^{-2}\text{W}$ ).

The power losses can be estimated by calculating the area under the curve. So, at balance condition the value of the power losses in the tower due to the eddy current is constant, while the shape of the induced current depends on the three sinusoidal current.

#### **4.3.7 Frequency of the excitation current**

It is a well-known fact that the eddy current is frequency dependent. Generally the transmission line are designed to operate at 50 or 60Hz which is the optimum frequency. That less than 50Hz may cause fluctuating in lights, and more than 60Hz the inductive loads will be high impedance, which require higher voltages for the same amount of current which draws a lot of difficulties in generating and transmitting the power. Now we calculated the eddy current in a small segment of the tower the power losses was found to be ( $P_e = 0.93 \times 10^{-2}\text{ W}$ ) for 60Hz system and ( $P_e = 0.64 \times 10^{-2}\text{W}$ ) for 50Hz power line system.

# CHAPTER FIVE

## CONCLUSIONS AND FUTURE WORK

### 5.1 Conclusion

The aim of the study is to investigate on the existence of eddy current in transmission towers due to power lines magnetic field under balanced condition. This eddy current may produce significant losses in the tower. In this study we presented a mathematical model for analyzing the eddy current in transmission towers that can be applied to any type of towers by segmenting the tower to small parts for the facilitation of the numerical calculation and to overcome the need of extra computational resources.

The frequency domain FDM is used to determine the low frequency magnetic field. The problem was simulated using MATLAB software.

It concluded that the induced eddy current depends on metals property, dimensions of the computational part of the tower (i.e. the shape of the tower), the distance to the source, frequency and the excitation current.

The results show that the eddy current is proportional to permeability and conductivity of the tower. The produced power losses due to the eddy current is linearly related to the excitation current. The study also shows that the design of the tower has a significant effect on the induced eddy current as different length for the cross arm was tested at the same current.



The importance of this research is that it offers important explanations to towers manufacturers in selecting the proper materials so that the eddy-current losses are minimum, in addition to the significance of the presented mathematical model to those interested in this field.

### **Future Work**

- Because of the limited computational resources it is not possible to estimate the eddy current losses in a real tower design, this might be done using another software to study the eddy current in a real design.
- It might be worthy to compare the simulated results with a practical result for eddy current in a metallic segment.

## References

1. Navani, J., N. Sharma, and S. Sapra, Technical and non-technical losses in power system and its economic consequence in Indian economy. *International Journal of Electronics and Computer Science Engineering*, 2012. 1(2): p. 757-761.
2. Kaune, W. and L. Zaffanella, Analysis of magnetic fields produced far from electric power lines. *IEEE Transactions on Power Delivery*, 1992. 7(4): p. 2082-2091.
3. Filippopoulos, G. and D. Tsanakas, Analytical Calculation of the Magnetic Field Produced by Electric Power Lines. *IEEE Transactions on Power Delivery*, 2005. 20(2): p. 1474-1482.
4. Zemljarić, B., Calculation of the Connected Magnetic and Electric Fields Around an Overhead-Line Tower for an Estimation of Their Influence on Maintenance Personnel. *IEEE Transactions on Power Delivery*, 2011. 26(1): p. 467-474.
5. Swanson, J., Magnetic fields from transmission lines: comparison of calculations and measurements. *IEE proceedings-Generation, Transmission and Distribution*, 1995. 142(5): p. 481-486.
6. Pathak, P., V. Kumar, and R. Vats, Harmful electromagnetic environment near transmission tower. *INDIAN JOURNAL OF RADIO AND SPACE PHYSICS*, 2003. 32(4): p. 238-244.
7. Atudori, M. and M. Rotariu, Electromagnetic radiation field near power lines and its environmental impact. *University" Politehnica" of Bucharest Scientific Bulletin, Series C: Electrical Engineering*, 2012. 74(1): p. 231-238.
8. Co, B.-K. and E.L.R. Gemmill, *Transmission Towers*. 1920: Blaw-Knox Company.
9. Lu, C., X. Ma, and J.E. Mills, Modeling of retrofitted steel transmission towers. *Journal of Constructional Steel Research*, 2015. 112: p. 138-154.

10. Kang, S.K.W., F. Albermani, and H. Lam, Modeling and Analysis of Lattice Towers with more accurate models. *Advanced Steel Construction*, 2007. 3(2): p. 565-582.
11. Preeti, C. and K.J. Mohan, Analysis of Transmission Towers with Different Configurations. *Jordan Journal of Civil Engineering*, 2013. 7(4): p. 450-460.
12. Gonen, T., *Electrical power transmission system engineering: analysis and design*. 2011: CRC Press.
13. Anumaka, M., Analysis of technical losses in electrical power system (Nigerian 330kV network as a case study). Department Of Electrical Electronic Engineering, Faculty of Engineering, Imo State University, Owerri, Imo State, Nigeria Email: engranumakamc@ yahoo. com, 2012.
14. Suriyamongkol, D., *Non-technical losses in electrical power systems*. 2002, Ohio University.
15. George, E., Intrasystem transmission losses. *Electrical Engineering*, 1943. 62(3): p. 153-158.
16. Gustafson, M. and J. Baylor, Approximating the system losses equation [power systems]. *IEEE Transactions on Power Systems*, 1989. 4(3): p. 850-855.
17. Davidson, I.E., et al., Technical loss computation and economic dispatch model for T&D systems in a deregulated ESI. *Power Engineering Journal*, 2002. 16(2): p. 55-60.
18. Olsen, R.G. and P. Wong, Characteristics of low frequency electric and magnetic fields in the vicinity of electric power lines. *IEEE Transactions on Power Delivery*, 1992. 7(4): p. 2046-2055.
19. Hameyer, K., R. Mertens, and R. Belmans, *Computation and measurement of electromagnetic fields of AC-high-voltage transmission lines*. 1996.
20. Garrido, C., A.F. Otero, and J. Cidras, Low-frequency magnetic fields from electrical appliances and power lines. *IEEE Transactions on Power Delivery*, 2003. 18(4): p. 1310-1319.

21. Molnar-Matei, F., et al. Double circuit 110 kV overhead line magnetic field analysis. in 2012 16th IEEE Mediterranean Electrotechnical Conference. 2012. IEEE.
22. Stangeland, K., Positioning in electromagnetic fields. 2015.
23. Sun, X., et al., Novel Application of Magneto-resistive Sensors for High-Voltage Transmission-Line Monitoring. IEEE Transactions on Magnetics, 2011. 47(10): p. 2608-2611.
24. Hamza, A.-S.H., Evaluation and measurement of magnetic field exposure over human body near EHV transmission lines. Electric Power Systems Research, 2005. 74(1): p. 105-118.
25. Sougui, A.O., Analysis and measurement of magnetic field emission near high voltage transmission lines (HVTL). 2014, Universiti Tun Hussein Onn Malaysia.
26. Hwang, C., Numerical computation of eddy currents induced in structural steel due to a three-phase current. Electric power systems research, 1997. 43(2): p. 143-148.
27. El Dein, A.Z., Calculation of the Electric Field Around the Tower of the Overhead Transmission Lines. IEEE Transactions on Power Delivery, 2014. 29(2): p. 899-907.
28. Zhao, T. and M.G. Comber, Calculation of electric field and potential distribution along nonceramic insulators considering the effects of conductors and transmission towers. IEEE Transactions on Power Delivery, 2000. 15(1): p. 313-318.
29. Al Salameh, M.S. and M. Hassouna, Arranging overhead power transmission line conductors using swarm intelligence technique to minimize electromagnetic fields. Progress in electromagnetics research B, 2010. 26: p. 213-236.
30. Ippolito, M.G., et al. Mitigation of 50 Hz magnetic field produced by an overhead transmission line. in Power Engineering Conference (UPEC), 2015 50th International Universities. 2015. IEEE.

31. Memari, A. and W. Janischewskyj, Mitigation of magnetic field near power lines. IEEE Transactions on Power Delivery, 1996. 11(3): p. 1577-1586.
32. Pettersson, P., Principles in transmission line magnetic field reduction. IEEE Transactions on Power Delivery, 1996. 11(3): p. 1587-1593.
33. Grigsby, L.L., Electric power generation, transmission, and distribution. Electric power engineering series, 2.; Electrical engineering handbook series, ed. R.C. Dorf. 2007: CRC Press 503\503.
34. Chari, M. and Z. Csendes, Finite element analysis of the skin effect in current carrying conductors. IEEE Transactions on Magnetics, 1977. 13(5): p. 1125-1127.
35. Elhirbawy, M., et al. Calculation of electromagnetic fields established by power transmission line using finite difference techniques. in Electrical and Computer Engineering, 2002. IEEE CCECE 2002. Canadian Conference on. 2002. IEEE.
36. Medved', D., Modeling of Electromagnetic Fields Close to the Very High Voltage and Extra High Voltage Poles. ELEKTROENERGETIKA, 2012. 5(2).
37. Hameyer, K., R. Mertens, and R. Belmans. Numerical methods to evaluate the electromagnetic fields below overhead transmission lines and their measurement. in Devices, Circuits and Systems, 1995., Proceedings of the 1995 First IEEE International Caracas Conference on. 1995. IEEE.
38. Liu, Y. and L.E. Zaffanella, Calculation of electric field and audible noise from transmission lines with non-parallel conductors. IEEE transactions on power delivery, 1996. 11(3): p. 1492-1497.
39. Bo, Z., et al., Electric field calculation for HV insulators on the head of transmission tower by coupling CSM with BEM. IEEE Transactions on Magnetics, 2006. 42(4): p. 543-546.
40. Budnik, K. and W. Machczyński, Contribution to studies on calculation of the magnetic field under power lines. European Transactions on Electrical Power, 2006. 16(4): p. 345-364.

41. CASE JR, R.L., Reducing Eddy Currents In High Magnetic Field Environments. 2008, University of Central Florida Orlando, Florida.
42. Chari, M., Finite-element solution of the eddy-current problem in magnetic structures. IEEE Transactions on Power Apparatus and Systems, 1974(1): p. 62-72.
43. Rodger, D. and J. Eastham, A formulation for low frequency eddy current solutions. IEEE Transactions on Magnetics, 1983. 19(6): p. 2443-2446.
44. Biddlecombe, C., et al., Methods for eddy current computation in three dimensions. IEEE Transactions on magnetics, 1982. 18(2): p. 492-497.
45. Simm, A., Quantitative interpretation of magnetic field measurements in eddy current defect detection. 2013.
46. Causon, D. and C. Mingham, Introductory finite difference methods for PDEs. 2010: Bookboon.
47. Bargallo, R., Finite elements for electrical engineering. Department of Electrical Engineering, Universitat Politecnica De Catalunya, 2006.
48. Chen, Q. and A. Konrad, A review of finite element open boundary techniques for static and quasi-static electromagnetic field problems. IEEE Transactions on Magnetics, 1997. 33(1): p. 663-676.
49. Sykulski, J., Computational magnetics. 2012: Springer Science & Business Media.
50. Oaten, S.R., Assessment of defects in ferromagnetic metals with eddy currents. 1989, Brunel University Institute for the Environment PhD Theses.
51. Chow, T.L., Introduction to Electromagnetic Theory: A Modern Perspective. 2006: Jones and Bartlett Publishers.
52. Sadiku, M.N.O., Elements of Electromagnetics. 2001: Oxford University Press.
53. Mur, G., Absorbing boundary conditions for the finite-difference approximation of the time-domain electromagnetic-field equations. IEEE transactions on Electromagnetic Compatibility, 1981(4): p. 377-382.

54. Amano, K., A charge simulation method for the numerical conformal mapping of interior, exterior and doubly-connected domains. *Journal of computational and applied mathematics*, 1994. 53(3): p. 353-370.



# CURRICULUM VITAE

## PERSONAL INFORMATION

**Name, surname:** Huda MOHAMMED

**Date and place of birth:** 5.10.1989- IRAQ

**E-mail:** hudajum@yahoo.com

## EDUCATION

**High School:** Alwasity High School, 2007

**B.Sc.:** University of Sulaymani, 2011

**M.Sc.:** The University Of Turkish Aeronautical Association, Electric and Electronic, 2017.

## Work Experience

Teaching Assistant at Alqalam University College, Engineering Department, 2011-2014.